

# UNIVERSITY OF VERONA

*DEPARTMENT OF*

*Medicine, Section of General Pathology*

*DOCTORAL SCHOOL OF*

*Life and Health Sciences*

*DOCTORAL PROGRAM IN*

*Inflammation, Immunity and Cancer*

*With the financial contribution of*

*University of Verona*

Cycle XXX

TITLE OF THE DOCTORAL THESIS

Coenzyme A synthase controls pathogenic features of myelin specific T cells by  
linking metabolic reprogramming to alteration of intracellular signaling pathways

S.S.D. MED/04

Coordinator: Prof. Gabriela Constantin

Signature 


Tutor: Prof. Gabriela Constantin

Signature 

Co-tutor: Dr. Barbara Rossi

Signature 

Doctoral Student: Dr. Tommaso Carlucci

Signature 

This work is licensed under a Creative Commons Attribution-Non Commercial-  
No Derivs 3.0 Unported License, Italy. To read a copy of the license, visit the web page:

<http://creativecommons.org/licenses/by-nc-nd/3.0/>



**Attribution** — You must give appropriate credit, provide a link to the license, and indicate if changes were made. You may do so in any reasonable manner, but not in any way that suggests the licensor endorses you or your use.



**Non Commercial** — You may not use the material for commercial purposes.



**No Derivatives** — If you remix, transform, or build upon the material, you may not distribute the modified material.

Coenzyme A synthase controls pathogenic features of myelin specific T cells by linking  
metabolic reprogramming to alteration of intracellular signaling pathways

Tommaso Carlucci  
PhD thesis  
Verona, 15/01/2018

## Table of contents

<b>Summary</b> .....	6
<b>Riassunto</b> .....	8
<b>Introduction</b> .....	11
1. <b>Autoimmunity</b> .....	11
1.1. <i>Introduction</i> .....	11
1.2. <i>Multiple sclerosis and its animal model:         experimental autoimmune encephalomyelitis</i> .....	13
2. <b>Immunometabolism</b> .....	15
2.1. <i>Immunometabolism: a novel frontier in immunology</i> .....	15
2.2. <i>T cell metabolism</i> .....	16
2.3. <b>CoA and its biosynthetic pathway</b> .....	20
2.3.1. <i>CoA</i> .....	20
2.3.2. <i>CoA biosynthesis pathway</i> .....	21
2.3.3. <i>Regulation of CoA levels</i> .....	22
2.3.4. <i>CoASY</i> .....	23
3. <b>Systems biology and -omics approaches</b> .....	24
<b>Materials and methods</b> .....	28
<i>Mice</i> .....	28
<i>Production of PLP<sub>139-151</sub>-specific encephalitogenic T cell lines</i> .....	28
<i>Pantethine preparation</i> .....	28
<i>Metabolomics analysis</i> .....	29
<i>Phosphoproteomics and network analysis</i> .....	29
<i>In vitro proliferation assay with PLP<sub>139-151</sub>-specific T cells</i> .....	30

<i>Bio-plex assay for cytokines detection .....</i>	31
<i>In vitro adhesion assay on purified integrin ligands.....</i>	32
<i>Silencing of CoASY expression in encephalitogenic T cells .....</i>	32
<i>CoASY quantification by Western blot analysis.....</i>	33
<i>In vitro proliferation assay with CoASY-silenced</i>	
<i>PLP<sub>139-151</sub>-specific T cells .....</i>	33
<i>Enrichment analysis of a PPI network centered on CoASY</i>	
<i>using a systems biology approach.....</i>	33
<i>EAE induction and in vivo treatment with pantethine.....</i>	34
<i>Statistics.....</i>	34
<b>Results .....</b>	36
<i>Actively proliferating PLP<sub>139-151</sub>-specific T cells display</i>	
<i>a metabolic profile distinct from resting T lymphocytes .....</i>	36
<i>CoA fueling inhibits anabolic metabolism in PLP<sub>139-151</sub>-specific</i>	
<i>effector T cells.....</i>	37
<i>Phosphoproteomics analysis elucidated the immuno-modulatory</i>	
<i>effect of CoA fueling in PLP<sub>139-151</sub>-specific encephalitogenic T cells .....</i>	41
<i>CoA fueling has immuno-modulatory effects on PLP<sub>139-151</sub>-specific T</i>	
<i>cells .....</i>	42
<i>Pantethine treatment inhibits proliferation of T cells in vitro.....</i>	42
<i>Pantethine treatment affects pro-inflammatory</i>	
<i>cytokines production of T cells in vitro .....</i>	43
<i>Pantethine treatment inhibits spontaneous adhesion</i>	
<i>of T cells in vitro.....</i>	43
<i>Silencing of CoASY abolished pantethine inhibitory effect</i>	
<i>in PLP<sub>139-151</sub> specific T CoA fueling.....</i>	44

<i>CoASY – RPS6KB1 complex links metabolism to immune related signaling pathways</i> .....	44
<i>Pantethine inhibits EAE development and ameliorates clinical outcome in established EAE</i> .....	45
<b>Discussion</b> .....	47
<b>Figures and tables</b> .....	54
<b>References</b> .....	83

## Summary

In recent years, it has become clear that metabolism critically influences the outcome of immune responses. Additionally, growing evidence suggest that changes in the metabolism of immune cells are associated with, and contribute to the pathogenesis of autoimmunity. Thus, the emerging field of immunometabolism may lead to the discovery of novel therapeutic targets for the treatment of autoimmune diseases. The involvement of aerobic glycolysis and other metabolic pathways in controlling the activation state of immune cells and the development of autoimmune diseases has been recently elucidated, but the effect of Coenzyme A (CoA) fueling in these pathologies never been studied thus far.

The **aim** of this study was to investigate the involvement of CoA synthase (CoASY), the enzyme that catalyzes the last two steps of CoA synthesis pathway, in the control of autoreactive myelin-specific T cell pathogenicity by using murine experimental autoimmune encephalomyelitis (EAE) as a model of autoimmune disease.

By using metabolomics and proteomics approaches and functional *in vitro* assays, we investigated the pathogenic features of autoreactive proteolipid protein (PLP)<sub>139-151</sub>-specific effector T cells, which represent major players in the pathogenesis of EAE in SJL mice.

Our metabolomics analysis showed that encephalitogenic (myelin-specific) T cells display reduced intracellular CoA synthesis, and increased levels of free fatty acids and glycolysis-, Krebs cycle- and pentose phosphate pathway-related metabolites, compared to resting T cells. We next investigated the immunomodulatory potential of the low molecular weight thiol pantethine, a CoA precursor, on the pathogenic features of encephalitogenic T cells and the impact of such immunomodulation on the development of EAE. CoA fueling, induced by pantethine treatment, reprogrammed autoreactive T cells, to a “resting-like state” leading to reduced glycolysis, blockade of pentose phosphate pathway, inhibition of nucleic acid synthesis, and significant alteration of lipid and protein content. The analysis of high throughput phosphoproteomics data revealed that pantethine

is able to affect crucial immune processes associated with the functionality and the pathogenicity of encephalitogenic T cells, such as cell activation and proliferation, cytokine production and cell migration. These observations were confirmed by functional *in vitro* assays showing that CoA fueling strongly affected encephalitogenic T cell functions by reducing their antigen-specific proliferative capacity, pro-inflammatory cytokine production and integrin-dependent adhesion *in vitro*. By using a genetic approach, we confirmed that pantethine induced the metabolic reprogramming of encephalitogenic T cells by potentiating the CoA synthesis pathway. Indeed, small interfering RNA (siRNA)-mediated silencing of CoASY led to a significant loss of the inhibitory effect induced by pantethine treatment on the proliferation rate of encephalitogenic T cells. Interestingly, the knockdown of CoASY in encephalitogenic T cells increased their proliferative capacity in absence of antigen stimulation, suggesting a key role of CoASY in the control of autoreactive T cell activation. Bioinformatics analysis using a systems biology approach revealed that CoASY, has a role in the regulation of immune-related signaling pathways such as mitogen-activated protein kinase (Mapk), Ras-related C3 botulinum toxin substrate 1 (Rac1) and mammalian target of rapamycin (mTOR) pathways. In light of these results, we finally tested the clinical potential of metabolic perturbation by pantethine *in vivo*. We found that pantethine treatment prevented the development of EAE by delaying the disease onset and reducing the clinical score. Furthermore, pantethine treatment started after disease onset significantly ameliorated disease course and severity.

In conclusion, our data demonstrate a new role for the CoA synthesis pathway in the metabolic reprogramming of autoreactive T cell necessary for their pathogenic features, suggesting that CoA fueling may represent a novel therapeutic approach for the treatment of autoimmune diseases.

## Riassunto

Negli ultimi anni è diventato sempre più chiaro come il metabolismo influenzi fortemente l'esito della risposta immunitaria. Inoltre, sono sempre più evidenti le associazioni tra i cambiamenti nel metabolismo delle cellule immunitarie e la patogenesi dell'autoimmunità. Pertanto, il campo di studio dell'“immuno-metabolismo” potrebbe portare alla scoperta di nuovi bersagli terapeutici per il trattamento delle malattie autoimmuni. Mentre l'importanza di vie metaboliche come la glicolisi aerobica nell'attivazione delle cellule del sistema immunitario e nello sviluppo delle malattie autoimmuni è già recentemente dimostrata, il ruolo del metabolismo del coenzima A (CoA) non è mai stato direttamente studiato in tali patologie.

Lo **scopo** di questo studio è stato quello di indagare il coinvolgimento della CoA sintasi (CoASY), l'enzima che catalizza gli ultimi due passaggi della via di sintesi del CoA, nell'attivazione e nelle funzioni patogeniche delle cellule T autoreattive mielina-specifiche e nella patogenesi dell'encefalomielite sperimentale autoimmune murina (EAE), usata nel nostro studio come modello di malattia autoimmune.

Attraverso l'applicazione di metodiche come la metabolomica, la proteomica e vari saggi funzionali *in vitro*, abbiamo investigato le caratteristiche patogenetiche delle cellule T effettrici PLP<sub>139-151</sub>-specifiche, che rappresentano i principali attori nella patogenesi dell'EAE nei topi di ceppo SJL.

L'analisi del profilo metabolico di tali cellule ha dimostrato che, rispetto alle cellule T resting, le cellule T encefalitogeniche (mielina-specifiche) presentano una riduzione della sintesi intracellulare di CoA ed un aumento nei livelli di acidi grassi e dei metaboliti relativi alla via della glicolisi, del ciclo di Krebs e del pentoso-fosfato. Alla luce di ciò, abbiamo studiato l'effetto immunomodulatore della pantetina, un tiolo a basso peso molecolare che agisce come precursore del CoA, sulle caratteristiche patogenetiche delle cellule T encefalitogeniche e l'impatto di tale immuno-modulazione sullo sviluppo dell'EAE. L'aumento di CoA, indotto dal trattamento con pantetina, ha



riprogrammato le cellule T auto-reattive, a uno "stato resting", riducendo la glicolisi, la via del pentoso fosfato, e la sintesi di acidi nucleici. Inoltre, abbiamo osservato alterazioni significative nel contenuto lipidico e proteico. L'analisi fosfoproteomica, ha rivelato che la pantetina è in grado di influenzare i processi immunitari necessari alla funzionalità e alla patogenicità delle cellule T encefalitogeniche, come l'attivazione e la proliferazione cellulare, la produzione di citochine pro-infiammatorie e la migrazione cellulare. Queste osservazioni sono state confermate da saggi funzionali *in vitro* che mostrano come l'aumento della sintesi di CoA riduce fortemente la capacità proliferativa antigene-specifica, la produzione di citochine pro-infiammatorie e l'adesione integrino-dipendente delle cellule T encefalitogeniche. Con un approccio genetico, abbiamo confermato che la riprogrammazione metabolica attuata dalla pantetina nelle cellule T encefalitogeniche, è dovuta ad un effettivo potenziamento della via di sintesi del CoA. Il silenziamento della CoASY ha infatti ridotto significativamente l'effetto inibitorio della pantetina sulla proliferazione delle cellule T encefalitogeniche. È interessante inoltre notare come la ridotta espressione della CoASY nelle cellule T encefalitogeniche abbia aumentato la loro capacità proliferativa in assenza di stimolazione antigenica, suggerendo un ruolo chiave della CoASY nel controllo dell'attivazione e delle funzioni delle cellule T autoreattive. L'analisi bioinformatica con un approccio di biologia dei sistemi ha rivelato che la CoASY può esercitare un ruolo diretto nella regolazione delle vie del segnale correlate alla risposta immunitaria, tra le quali, le vie di Mapk, Rac1 e mTOR. Alla luce del significativo effetto metabolico e immuno-modulatore *in vitro* del potenziamento del CoA nelle cellule T encefalitogeniche, abbiamo testato *in vivo* il potenziale clinico della pantetina in un modello di patologia autoimmune come l'EAE. Il trattamento con la pantetina in fase pre-clinica ha inibito lo sviluppo dell'EAE ritardando l'insorgenza della malattia e la sua severità. Inoltre, il trattamento con la pantetina, iniziato dopo l'insorgenza della malattia, è stato in grado di migliorarne il decorso clinico e ridurne significativamente la gravità.

In conclusione, i nostri dati dimostrano un nuovo ruolo della via di sintesi del CoA nella riprogrammazione metabolica delle cellule T autoreattive

necessaria allo svolgimento delle loro funzioni patogenetiche, suggerendo che il potenziamento del metabolismo del CoA nei linfociti autoreattivi potrebbe rappresentare un nuovo bersaglio terapeutico per il trattamento di patologie autoimmuni.

# Introduction

## 1. Autoimmunity

### 1.1 Introduction

The immune system continuously protects the human body from infectious diseases and tissue insults, avoiding excessive inflammatory reactions and damage. Multiple, non-redundant checkpoints are in place to prevent such potentially deleterious autoimmune responses while preserving protective immunity against foreign pathogens. Nevertheless, a large and growing segment of the population is developing autoimmune diseases. If mechanisms controlling this system fail, immune cells attack the body's own tissue and autoimmune diseases such as rheumatoid arthritis (RA), multiple sclerosis (MS) or type 1 diabetes (T1D) develop. The vast majority of autoimmune diseases develop as a consequence of complex mechanisms that depend on genetic, epigenetic, molecular, cellular, and environmental elements and result in alterations in many different immune checkpoints, and ultimately in the breakdown of immune tolerance. The consequences of this breakdown are harmful inflammatory responses in peripheral tissues driven by innate immunity and self-antigen-specific pathogenic T and B cells.

T cells play a central role in the regulation and initiation of these responses, and mechanisms such as central and peripheral tolerance are necessary to control autoreactive T cell activation. Central tolerance eliminates potentially autoreactive lymphocytes that develop in the thymus by subjecting thymocytes with high affinity for self-antigens to either clonal deletion (negative selection) or selection into the regulatory T (Treg) lineage. Many autoreactive T cells escape this checkpoint and can be found in the peripheral blood of healthy individuals; however, these self-reactive cells are not sufficient to induce autoimmunity due to additional controls by peripheral tolerance mechanisms (Reijonen et al., 2002; Su et al., 2013; Wucherpfennig et al., 1994; Zhang et al., 2008). Peripheral tolerance is achieved through T cell-intrinsic mechanisms that lead to clonal deletion, anergy, or immunological ignorance as well as extrinsic control by specialized

populations of suppressor cells that regulate potentially harmful responses of autoreactive T and B cells (Bluestone, 2011; Bour-Jordan et al., 2011).

A growing body of work suggests that autoreactive T cells have unusual binding properties for their cognate major histocompatibility complex (MHC)-peptide ligands. Autoreactive T cells with unusual T cell receptor (TCR) topologies may escape thymic deletion due to aberrant/reduced binding to the MHC that is insufficient to trigger apoptosis (Wucherpfennig et al., 2009). Structural analyses of TCRs from patients with MS and T1D have revealed this property of autoreactive TCRs specific for disease-related self-peptides, such as myelin basic protein and insulin (Bulek et al., 2012; Hahn et al., 2005).

Classically, the immune response to an antigen, including self-antigens, is initiated when specialized antigen-presenting cells, such as dendritic cells (DCs), take up and process an antigen, become activated and present it to resting CD4<sup>+</sup> T cells. T cells with a TCR specific for that antigen begin to proliferate and differentiate into particular T-helper cell subsets (e.g. Th1, Th2, Th17), which help to establish humoral as well as cellular immunity. Under healthy conditions, those pro-inflammatory T cells are counterbalanced by anti-inflammatory Foxp3<sup>+</sup> Treg cells. Autoimmunity occurs when tolerance to self-antigens is broken. Particularly, a contribution of Th1 or Th17 cells to autoimmune pathology is widely accepted for diseases such as RA, MS and T1D. Importantly, Tregs are absolutely essential for maintaining peripheral tolerance as Treg depletion in newborn mice causes fatal generalized autoimmunity (Kim et al., 2007).

The prevalence of autoimmune disorders is currently estimated to be >5% worldwide, with a dramatic increase in the incidence during the last decade (Bach, 2002). Importantly, this increase in autoimmune disease appearance generates significant socio-economic expenses. In Europe, the annual burden through treatment costs and early retirements is estimated to be >15 billion Euros (Freitag et al., 2016). For these reasons, a better understanding of the pathogenesis of autoimmune diseases is needed, which may lead to the development of new therapeutic strategies without severe adverse effects and covering the high percentage of non-responders to current drugs.

## *1.2 Multiple sclerosis and its animal model: experimental autoimmune encephalomyelitis*

MS is one of the most common causes of neurological disability in young adults between the ages of 20 and 40 years. It is a chronic inflammatory autoimmune demyelinating disease of the central nervous system (CNS) characterized by inflammatory and degenerative changes in the brain and spinal cord (SC). MS is characterized by multifocal perivascular inflammatory infiltrates, predominantly lymphocytes and macrophages, which cause myelin breakdown and axonal degeneration. Pathogenesis of MS is also characterized by loss of the blood brain barrier (BBB) integrity and migration of autoreactive T-cells and monocytes. The etiology of MS is still unknown, but there is strong evidence that genetic predisposition associated with environmental factors and autoimmunity plays a major role in disease pathogenesis. Progressive disability is caused by inflammation in areas of the white matter of the CNS, followed by destruction of myelin in the brain and SC. Clinical symptoms of MS include motor dysfunction, fatigue, tremor, nystagmus, acute paralysis, loss of coordination or balance, numbness, disturbances in speech and vision and cognitive impairment (Ortiz et al., 2014). The cause of the recurrent inflammation in MS is now generally accepted to be autoimmune in nature. Studies demonstrating the presence of inflammatory cells and their products in the brain lesions of MS patients, in addition to reports from animal models, has led to the generally accepted hypothesis that disease is mediated by pathogenic T cell responses against myelin antigens, followed by a broader neurodegenerative process (Compston and Coles, 2008). Leukocyte infiltration from peripheral circulation through the BBB causes the activation of microglia and astrocytes leading to the myelin sheath and the underlying axon damage.

The most widely used animal model of autoimmunity is EAE (Gold et al., 2006; Zamvil and Steinman, 1990). Specifically, EAE represents the animal model of MS (Dendrou et al., 2015). EAE can be induced by immunization of susceptible experimental animal strains including primates and rodents with myelin autoantigens emulsified in complete Freund's adjuvant (CFA) or by adoptive transfer of T cells specific for brain antigens (Ben-Nun et al., 1981). A

conceptual breakthrough, indeed, was achieved in the 1980s by the groups of Wekerle and Cohen, who showed that myelin-specific CD4<sup>+</sup> T cell lines propagated *in vitro* could, upon adoptive transfer, induce demyelinating inflammation in the CNS parenchyma (Ben-Nun et al., 1981). This proved that EAE is induced by an autoimmune response to myelin antigens initiated by CD4<sup>+</sup> T cells. Thus, EAE represents an invaluable tool to study the activation of autoreactive T cells in the peripheral immune compartment, their migration into the CNS and their reactivation, and subsequent inflammation in the target tissue (**Figure 1**).

The best characterized myelin-derived autoantigens are PLP, myelin basic protein (MBP), myelin oligodendrocyte glycoprotein (MOG), and myelin-associated oligodendrocyte basic protein (MOBP) (Gold et al., 2006). Currently, the most common protocol for EAE induction is based on the injection of an encephalitogenic peptide, usually MOG<sub>35-55</sub> or PLP<sub>139-151</sub>, which is emulsified in CFA containing mineral oil and *Mycobacterium tuberculosis* strain H37Ra, followed by injection of pertussis toxin. Depending on the immunization protocol and genetic background of the mouse strain, EAE can develop with an acute, chronic progressive or relapsing–remitting course (Steinman, 1999). Moreover, the main inducers of EAE, i.e. myelin antigen-specific T cells, also called encephalitogenic T cells, obtained from lymph nodes and spleens of mice immunized with myelin antigens (Piccio et al., 2002), can be studied *in vitro* by standard immunological techniques such as proliferation assays, adhesion assays, surface marker analysis by flow cytometry, gene silencing and by advanced high throughput “-omics” approaches such as metabolomics and proteomics (Hasin et al., 2017).

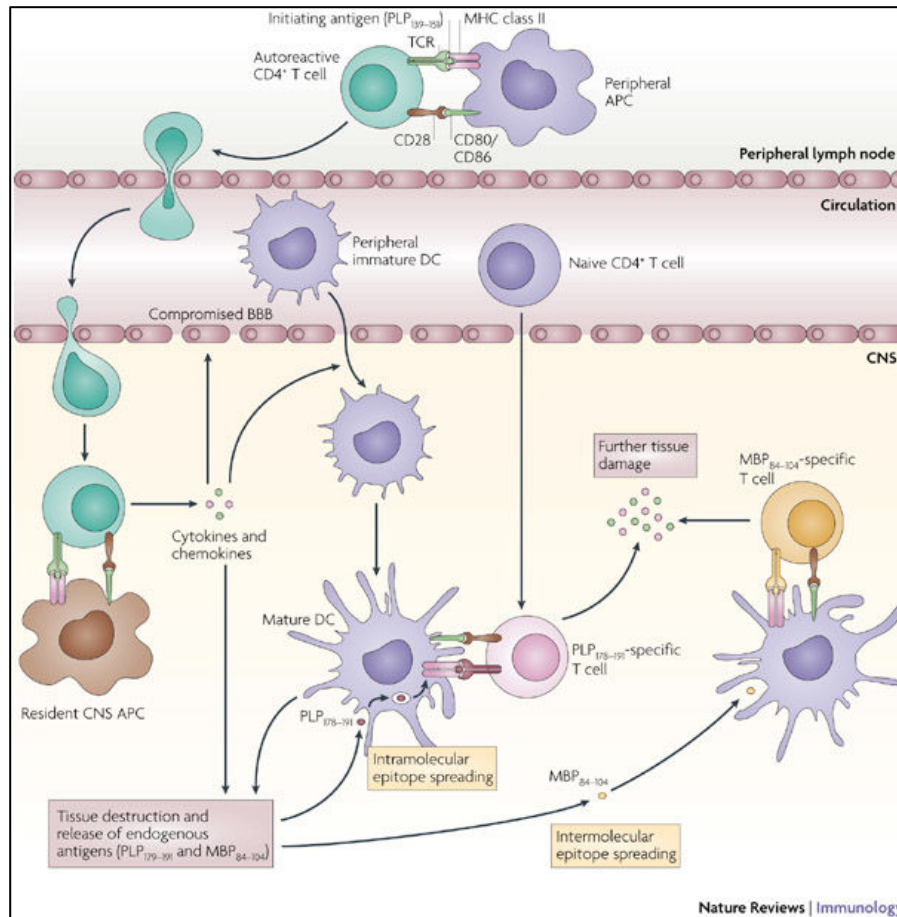


**Figure 1. CNS and lymph node activation of myelin-specific CD4<sup>+</sup>T cells.** (Picture adapted from Miller et al., 2007)

## 2. Immunometabolism

### 2.1 Immunometabolism: a novel frontier in immunology

Immunometabolism bridges the historically independent disciplines of biochemistry and immunology, and represents a novel field of investigation that links immune cell activation and functions with the biochemical changes correlated with their intracellular metabolic state. The field of immunometabolism was firstly introduced in the early '80s, when pioneering studies demonstrated that inflammation plays a crucial role in the development of obesity and metabolic disorders. In obese individuals, metabolic tissues (adipose tissue and liver) are infiltrated by activated immune cells, which produce detrimental pro-inflammatory mediators that impair glucose and lipid homeostasis. Interestingly, blocking inflammatory pathways (e.g. anti-TNF therapy) inhibits the generation

of correlated metabolic disorders (Hotamisligil, 2017). In the last two decades, many studies demonstrated that immune cells regulate the generation, strength, and duration of immune responses by fine-tuning their intracellular metabolic profile.

The activation, growth and proliferation, engagement of effector functions, and return to homeostasis of immune cells are intimately linked and dependent on dynamic changes in cellular metabolism. The utilization of particular metabolic pathways is controlled on one level by growth factors and nutrient availability dictated by competition between other interacting cells and on another level by the exquisite balance of internal metabolites, reactive oxygen species (ROS), and reducing and oxidizing substrates. The study of immune cells, particularly lymphocytes and myeloid cells, has lent deep insight into how cells differentiate and coordinate their behaviors with metabolism under a wide array of settings. Activation of immune cells in response to infection is the result of the summation of antigen-induced gene-expression programs integrated with environmental signals. Both innate and adaptive immune cells increase their metabolic throughput upon stimulation, promoting energy generation and biosynthesis, while shifting the relative usage of metabolic pathways to support proliferation, effector molecule production, and differentiation (O'Neill and Pearce, 2016; MacIver et al., 2013; Pollizzi and Powell, 2014; Buck et al., 2015). Moreover, alteration of metabolic pathways in specific immune cell subsets can impair their activation, polarization and faith leading to a strong modulation of inflammatory responses. These metabolic pathways, although diverse in terms of their end products, are closely linked as a consequence of shared fuel inputs, and a reliance on products from one pathway to feed into alternative pathways as key synthetic precursors (reviewed in O'Neill et al., 2016).

## *2.2 T cell metabolism*

Immune cells have different metabolic requirements depending on diverse environmental cues, their activation and differentiation state (Buck et al., 2015; Lochner et al., 2015). In order to cope with their basic requirements for survival, resting leukocytes rely on the Krebs cycle and subsequent oxidative



phosphorylation (OXPHOS), yielding ATP and CO<sub>2</sub>. Furthermore, they generate energy by degrading lipids during fatty acid oxidation (FAO) (Michalek et al., 2011) (**Figure 2**). Upon activation, immune cells change their metabolic profile. Specifically, in order to meet the enhanced demands subsequent to activation and upon differentiation of naïve T cells into effector lineages (e.g. Th1, Th2, Th17), T cells rely on the activation of mTOR. This serine-threonine kinase guides T cell differentiation and function (Waickman and Powell, 2012). mTOR integrates two signaling complexes, mTOR complex 1 (mTORC1) and mTOR complex 2 (mTORC2), that are composed of different regulatory subunits and possess distinct activation patterns. mTORC1 is induced after TCR-CD3/CD28-mediated stimulation of the phosphoinositide 3-kinase (PI3K)/AKT pathway. Activation of mTORC1 induces a metabolic switch in T cells in order to supply building blocks for cell proliferation and differentiation. T cells switch to glutaminolysis and aerobic glycolysis, the so-called Warburg effect characterized by glucose fermentation into lactate, a process that occurs despite the presence of sufficient oxygen to support mitochondrial OXPHOS (Rathmell et al., 2000; Roos and Loos, 1973). In order to provide lipids for the assembly of membranes, fatty acid synthesis (FAS) is increased with a respective decrease in FAO (Berod et al., 2014) (**Figure 2**). Instead, memory T cells and Foxp3<sup>+</sup> Tregs rely on mitochondrial FAO rather than employing FAS (Michalek et al., 2011) (**Figure 2**). ROS such as superoxide, hydrogen peroxide or hydroxyl radicals are produced as a result of energy-generating pathways and it is important to maintain redox balance during all metabolic reactions occurring in the cell, that is, to keep balance between ROS and antioxidants being able to scavenge ROS (Nathan and Cunningham-Bussel, 2013). Maintaining redox balance is of particular importance since ROS are able to oxidize protein thiols and may therewith affect proper protein functioning.

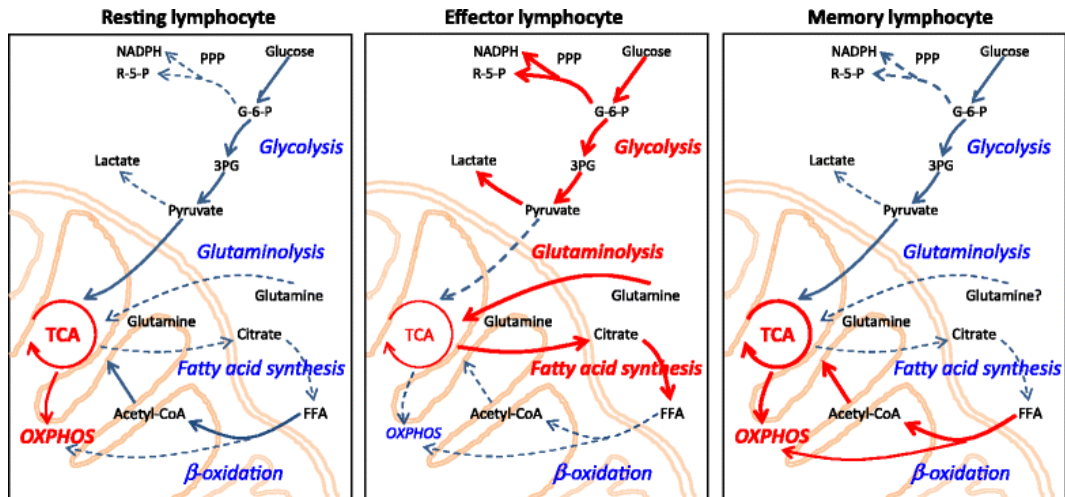


**Figure 2. Metabolic pathways match T cells' functional demands.** Schematic diagrams of metabolic pathways employed by T cells at different stages of activation and differentiation. Dominant pathways are indicated as red cascades. Blue arrows show pathways that are used at a steady level, and dashed arrows indicate pathways that might be utilized but are insufficiently investigated. (Left) Resting lymphocytes generate energy from glucose, fatty acids and amino acids. Most ATP is produced in mitochondria by fermentation of acetyl-CoA in the Krebs cycle (also known as tricarboxylic acid (TCA) cycle) and OXPHOS. (Middle) Effector lymphocytes (activated lymphocytes) swiftly and massively upregulate glycolysis and glutaminolysis, while keeping the TCA cycle low. These cells switch lipid metabolism from beta-oxidation towards FAS (lipogenesis). (Right) Memory lymphocytes mainly use beta-oxidation to support their energy needs. 3PG, 3-phosphoglycerate; FFA, free fatty acid; G-6-P, glucose-6-phosphate; NADPH, nicotinamide adenine dinucleotide phosphate; PPP, pentose phosphate pathway; R-5-P, ribose 5-phosphate. (Picture adapted from Yang et al., 2015).

Recent studies demonstrated that interfering with metabolic checkpoints in T cells such as FAS prevents autoimmunity in a murine model of MS (Berod et al., 2014) demonstrating a link between immunometabolism and autoimmunity. This connection has important implications: (i) a particular T-cell response may be shaped by the presence of defined metabolic end products (Barbi et al., 2013) and (ii) understanding common alterations in metabolic pathways, irrespective of the underlying autoimmune disorder, opens up the possibilities for the identification of both novel biomarkers and therapeutic strategies (Yang et al., 2015).

As the details of how metabolic reprogramming regulates immune function are revealed, new potential targets for modulating immune responses have emerged (reviewed in (Patel and Powell, 2017)). For example, the drug

rapamycin, an inhibitor of mTOR pathway (**Figure 3**), is able to slow down T cell proliferation (Sigal and Dumont, 1992) but also to promote Treg generation and T cell anergy (Battaglia et al., 2005; Powell et al., 1999). The small molecule inhibitor DON (6-Diazo-5-oxoL-norleucine), which is a glutamine antagonist, potently inhibits glutamine-dependent metabolism and T cell responses (Thomas et al., 2014) (**Figure 3**). Given the importance of increased glycolysis in the activation of effector T cells, the inhibitor of glycolysis 2-deoxy-glucose (**Figure 3**) was found to markedly diminish disease in a model of EAE (Shi et al., 2011). The enhancement of pyruvate conversion to acetyl-CoA, by the inhibition of pyruvate dehydrogenase kinases (PDHK) with dichloroacetate (DCA) in mice (**Figure 3**), markedly diminished disease pathology in EAE, by a promotion of Treg generation with enhanced OXPHOS and by the inhibition of effector T cells by suppressing glycolysis (Gerriets et al., 2015).

To note, accumulating evidence suggests that, although manifesting in different clinical forms, some human autoimmune diseases display common alterations in metabolic pathways, key metabolites and metabolic byproducts such as ROS. Other examples for metabolic changes in autoimmune settings include modifications in amino acid and cholesterol levels or glucose catabolism (Freitag et al., 2016).

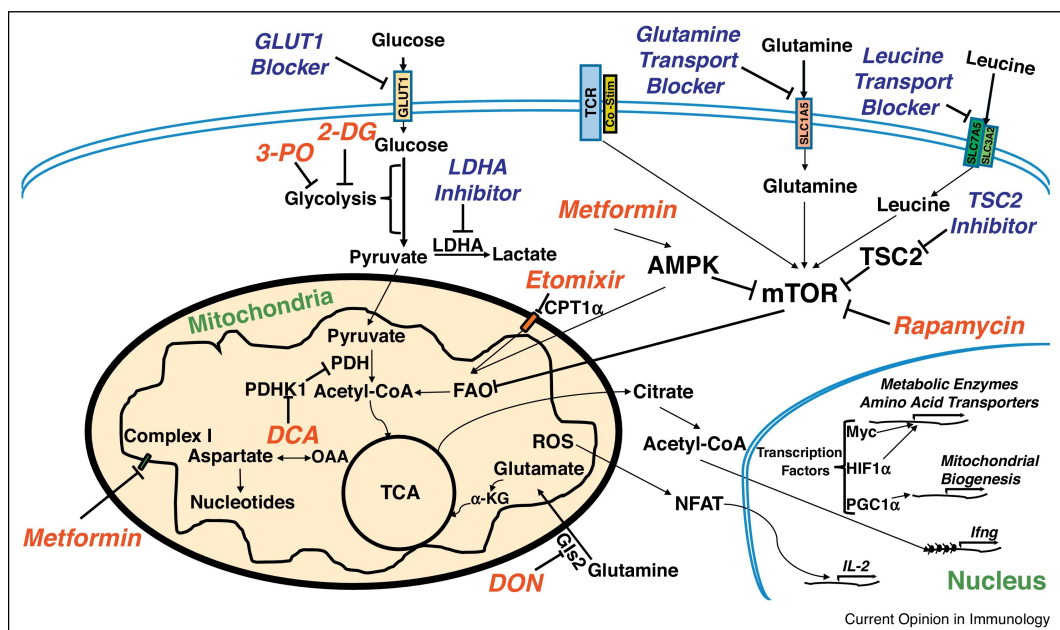


**Figure 3. Targeting metabolism to regulate T cell function.** In as much as T cell activation, differentiation and function is intimately linked to metabolism, targeting metabolism is emerging as a novel means of regulating T cell responses. Red highlights metabolic inhibitors that have been successfully employed to modulate T cell function. In blue are potential therapeutic targets based on the role of metabolic programs already well studied. (Picture adapted from Patel and Powell, 2017).

## 2.3 CoA and its biosynthetic pathway

### 2.3.1 CoA

CoA is an essential, universally distributed, thiol-containing cofactor that works as the major acyl group carrier in all cells. This molecule is involved in hundreds of reactions and is required for the metabolism of fatty acids, carbohydrates, amino acids and ketone bodies. CoA is a major regulator of energy metabolism, although it is often overlooked. Acetyl-CoA in particular is strategically positioned at the crossroads of energy metabolism. Just like all the roads lead to Rome, both anabolic and catabolic pathways converge at the formation of this small molecule, yet acetyl-CoA maintains order by reinforcing the partition of pyruvate between synthesis and degradation through its differential regulation of pyruvate dehydrogenase and carboxylase. Traffic control beyond this metabolic junction is exerted by acetyl- and other acyl-CoAs through both allosteric and post-translational regulation. Acetyl-CoA, for example, is used to modify enzymes, transcription factors and chromatin covalently and reversibly to govern their activities (Cai et al., 2011; Lundby et al., 2012; Siudeja et al., 2011). These ingenious mechanisms coordinate the expression and activity of a multitude of enzymes and processes with the energy state of the cell. Thus, CoA and a few other small molecules like NAD<sup>+</sup> and ATP can act as global regulators of cellular metabolism both together with and independent from the action of key transcription factors. Consistent with these key functions, CoA levels are flexible in cells so that the available supply is sufficiently adaptive to metabolic challenge.

In order for CoA to regulate such diverse cellular functions, its biosynthesis, CoA/CoA thioester ratio and degradation must be tightly regulated in different cellular compartments. There are several possibilities to consider for regulatory mechanisms, including (i) regulation of gene expression for the biosynthetic enzymes; (ii) post-translational modifications and activity regulation

of CoA biosynthetic enzymes; (iii) changes in the compartmentalization; (iv) metabolic flux of CoA and its thioester derivatives; and (v) degradation of CoA (Leonardi et al., 2005).

### 2.3.2 CoA biosynthesis pathway

In all living organisms, CoA synthesis is initiated with pantothenate, which is more commonly known as vitamin B5. Plants, fungi and most bacteria can synthesize pantothenate *de novo* and only animals and some microbes need to obtain it from outside. CoA is synthesized in a five-step process that requires four molecules of ATP, one of pantothenate and one of cysteine. (Leonardi et al., 2005):

1. Pantothenate is phosphorylated to 4'-phosphopantothenate by the enzyme pantothenate kinase (PanK). This is the committed step in CoA biosynthesis and requires ATP. Moreover, this step has been shown to be rate-limiting in most organisms and subjected to feedback regulation by CoA itself or its derivatives (Rock et al., 2000).
  2. A cysteine is added to 4'-phosphopantothenate by the enzyme phosphopantothenoylcysteine synthetase (PPCS) to form 4'-phospho-N-pantothenoylcysteine (PPC). This step is coupled with ATP hydrolysis.
  3. PPC is decarboxylated to 4'-phosphopantetheine by phosphopantothenoylcysteine decarboxylase (PPCDC).
  4. 4'-phosphopantetheine is adenylated to form dephospho-CoA by the phosphopantetheine adenylyl transferase (PPAT) activity of the bifunctional enzyme CoASY. This step represents the second rate-limiting reactions in the pathway.
  5. Finally, dephospho-CoA is phosphorylated to CoA by the dephospho-CoA kinase (DPCK) activity of CoASY. This final step requires ATP.
- (All steps reviewed in Leonardi and Jackowski, 2007).

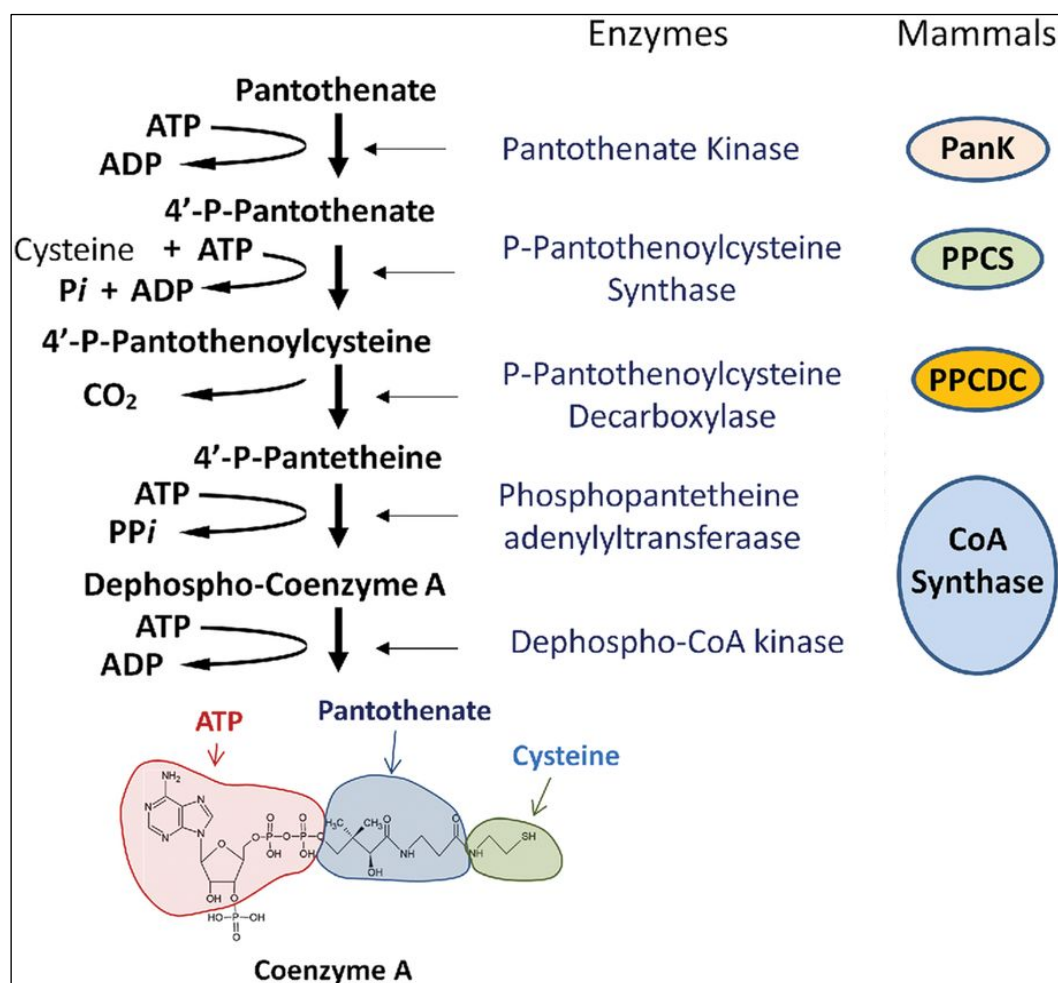


**Figure 4. Schematic diagram of a universal pathway for CoA biosynthesis and its key players in mammals.** The commitment step is the phosphorylation of pantothenate (vitamin B5) by PanK to 4'-phosphopantothenate. This is followed by condensation with cysteine catalyzed by PPCS and then decarboxylation to form 4'-phosphopantetheine by PPCDC. 4'-Phosphopantetheine is adenylylated to dephospho-CoA by PPAT, then phosphorylated by DPCK at the 3'-hydroxy group of the ribose to form CoA. In mammals, the last two steps are catalyzed by a single bifunctional polypeptide, CoASY. (Picture adapted from Martinez et al., 2014).

### 2.3.3 Regulation of CoA levels

The levels of CoA and its thioesters derivatives are tightly regulated by various extracellular stimuli, including hormones of metabolic homeostasis, nutrients, intracellular metabolites and stress. It has long been known that fasting, glucagon and glucocorticoids, and treatment with lipid-lowering drugs can increase the total level of CoA (Berge et al., 1983; Horie et al., 1986; Kerbey et al., 1977; Reibel et al., 1981; Smith and Savage, 1980). On the other hand, insulin,

glucose, fatty acids and pyruvate were shown to decrease the level of intracellular CoA (Berge et al., 1984; Robishaw et al., 1982). Change in the level of CoA were also reported in several pathologies, such as diabetes, Reye's syndrome, cancer, vitamin B12 deficiency, cardiac hypertrophy and neurodegeneration with brain iron accumulation (Brass et al., 1990; Corkey et al., 1988; Dusi et al., 2014; Hörtnagel et al., 2003; Kerbey et al., 1977; McAllister et al., 1988; Reibel et al., 1981, 1983; Zhou et al., 2001). The molecular mechanisms implicated in the regulation of intracellular level of CoA and the CoA/CoA derivatives ratio are not well understood. To date, most studies mainly focused on studying the regulation of the two rate-limiting enzymes in CoA biosynthesis, PanK and CoASY.

From bacteria to mammalian cells, negative-feedback regulation of PanK, and hence CoA biosynthesis, by CoA, acetyl-CoA, acyl-CoA is a well-documented fact (Begley et al., 2001; Dusi et al., 2014; Hörtnagel et al., 2003; Kleinkauf, 2000; Leonardi et al., 2005; Rock et al., 2000; Zhou et al., 2001). Taking into account that the intracellular levels of CoA/CoA derivatives levels are regulated by hormones, nutrients and intracellular metabolites, the research on the cross-talk between signal transduction pathways and CoA biosynthetic enzymes has been recently initiated.

#### 2.3.4 *CoASY*

To date, mammalian CoASY was found to be in complex with different proteins implicated in diverse signaling pathway, including ribosomal protein serine 6 kinase 1 (RPS6K1) (Nemazanyy et al., 2004), p85 $\alpha$  regulatory subunit of PI3K (phosphoinositide 3-kinase) (Breus et al., 2009), tyrosine phosphatase Shp2PTP (Src homology 2 domain-containing protein tyrosine phosphatase), tyrosine kinase Src (Breus et al., 2010), and ECD4 (enhancer of mRNA-decapping protein 4) (Gudkova et al., 2012). Some of these interactions were shown to be modulated by serum starvation/activation and in response to stresses. On the other hand, the activity and function of CoASY was also found to be regulated by post-translational modifications. For example, tyrosine phosphorylation of CoASY by members of the Src tyrosine kinase family was shown to be required for its interaction with p85 $\alpha$  regulatory subunit of PI3K

(Breus et al., 2009). Moreover, tyrosine dephosphorylation of CoASY by Shp2PTP in vitro results in the increase of its PPAT activity (Breus et al., 2010). The interaction of CoASY with ECD4, a central scaffold component of processing bodies, is regulated by growth factors and is affected by cellular stresses (Gudkova et al., 2012). EDC4 was also shown to strongly inhibit the dephospho-CoA kinase activity of CoASY in vitro (Gudkova et al., 2012).

The importance and mechanisms of these interactions are not well understood but might be important for the formation of a potential CoA biosynthetic complex.

### **3. Systems biology and -omics approaches**

Systems Biology is an inter disciplinary field that takes great advantage of network-based approaches to model and study complex biological processes (Ideker et al., 2001). Classic biology is, and historically was, focusing on single biological entities like, for instance, a protein. The innovative perspective that the systems biology approach proposes is the analysis of what happens when different actors play their role together, giving rise to complex systems. This goal is achieved by considering the set of all the interactions that take place between these objects in order to build and model a system. The system can finally be exploited by investigating (i) the role of each single actor and also, more interestingly, (ii) the emergent properties that arise because of their interactions. This is a new and very promising approach, which gives us the possibility to obtain a comprehensive view of complex biological systems like, for instance, an immune cell (Barabási and Oltvai, 2004). Systems biology is a mixture of very different techniques, skills and technologies and requires knowledge from very different fields (**Figure 4**). Genetics, genomics, proteomics, metabolomics and transcriptomics (-omics approaches) are current high throughput technologies that generate a very large amount of data (Hasin et al., 2017) (**Figure 4**). Mathematical skills are required to define and build the systems of interacting actors (Lango Allen et al., 2010; Li et al., 2002). Statistical techniques are used to investigate the data and to test the hypothesis and results (**Figure 4**). Finally, information technologies play a very important role since they allow managing the big amount



of data, to extract useful information through algorithms and to visualize models and results in a meaningful way and, especially, in a human-readable format.

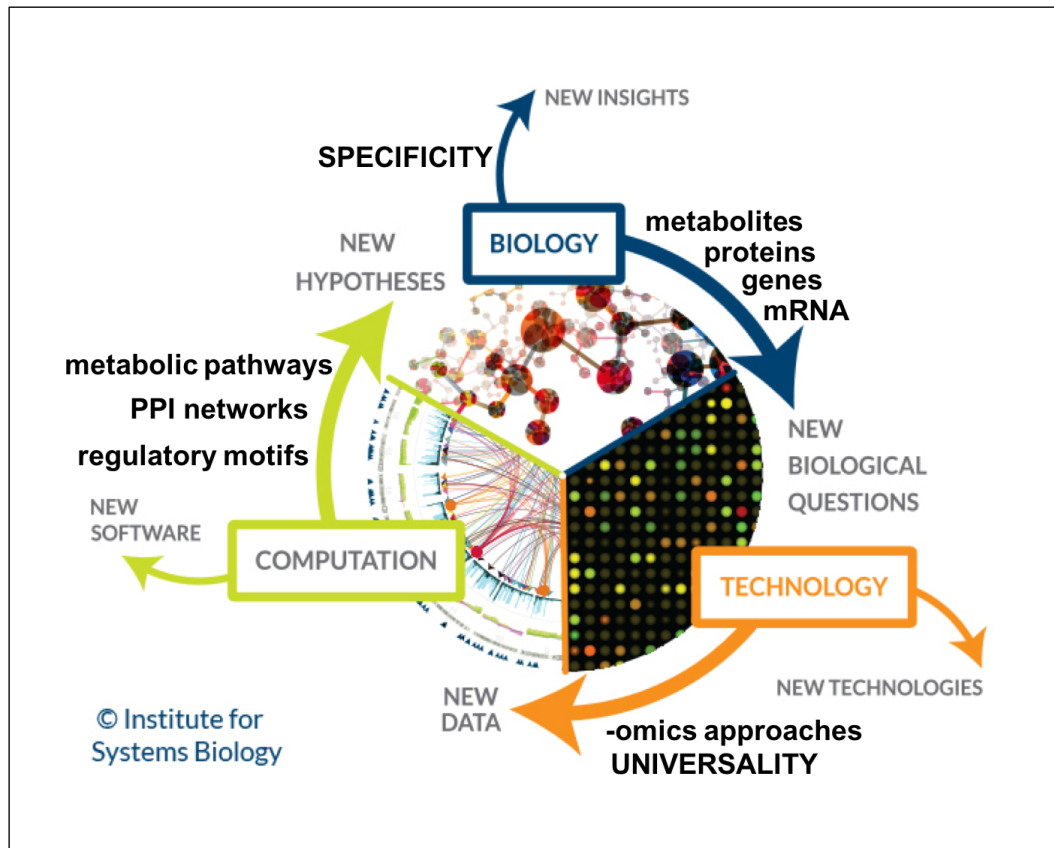


**Figure 5. The systems biology flow.** Reductionism, which has dominated biological research for over a century, has provided a wealth of knowledge about individual cellular components and their functions. Despite its enormous success, it is increasingly clear that a discrete biological function can only rarely be attributed to an individual molecule. Instead, most biological characteristics arise from complex interactions between the cell’s numerous constituents, such as proteins, DNA, RNA and metabolites. Therefore, a key challenge for biology in the twenty-first century is to understand the structure and the dynamics of the complex intercellular web of interactions that contribute to the structure and function of a living cell. The development of high-throughput data-collection techniques (-omics approaches), as epitomized by the widespread use of microarrays or mass spectrometry, allows for the simultaneous interrogation of the status of a cell’s components at any given time. In turn, new technology platforms, help to determine how and when these molecules interact with each other. Various types of interaction networks (including protein–protein interaction, metabolic, signaling and transcription-regulatory networks) emerge from the sum of these interactions and can be visualizes and analyzed thanks to bioinformatics computational software in order to generate new hypothesis, which can be studied in detail. (Integrated figure from Systems Biology Institute of Seattle: “systemsbiology.org/about/what-is-systems-biology/)

Bioinformatics and computational biology are the natural conjugations of the skills that are considered necessary to investigate all the complexity that comes from this amount of information. There are many different methodologies to exploit all the data produced by the modern -omics techniques and it is possible to find many software packages, web services and programming languages. There are also many biological databases that we can easily access to download protein structures, sequenced genomes, biological and disease networks, ontologies, standardized names and so on: STRING (Szklarczyk et al., 2017), GeneOntology (Ashburner et al., 2000) and Kegg (Kanehisa and Goto, 2000; Kanehisa et al., 2014) are just very few examples.

Systems biology represents the modern transition from a reductionist to a holistic view of biology. Reductionism is, and was, the main method used to address biological problems but things seem to be changing. Some scientists in the past and an increasing number of researchers today are considering biology as a set of interacting objects that should be considered together. In this sense, the holistic approach is (re)gaining more and more interest and an interdisciplinary knowledge that crosses different fields like, for instance, mathematics and biology, is becoming more and more important.

A very interesting, current, model that allows investigating biological systems properties takes advantage of graph theory. Networks, or graphs, are mathematical abstractions that could be used to model complex biological systems. Biological networks are composed by different kinds of actors that may be metabolites, genes, RNAs, and proteins (Alon, 2003) (**Figure 5**). From a mathematical perspective, networks, abstracted as graphs, are sets of objects that are used to describe interactions, called edges, between actors, called nodes. Formally a graph is defined as  $G = (E; V)$  where  $E$  is a set of edges and  $V$  the set of vertexes, i.e. the nodes. This simple notation is very useful to model complex, static biological processes where hundreds of genes, RNAs, proteins and metabolites interact together generating thousands of connections (Pastrello et al., 2014) (**Figure 5**). This static representation gives us a frame of the cell. It is not able to take into account the time, which means that the interactions do not change

over time. But graphs can be used to represent dynamic processes. These dynamic models permit to describe a changing system and the kinetics that take place, for instance, inside a cell. Some of these models are (i) Petri-nets (Goss and Peccoud, 1998), (ii) P-systems (Păun, 2000) and (iii)  $\pi$ -calculus models (Regev et al., 2001) just to cite few interesting methodologies in the field.

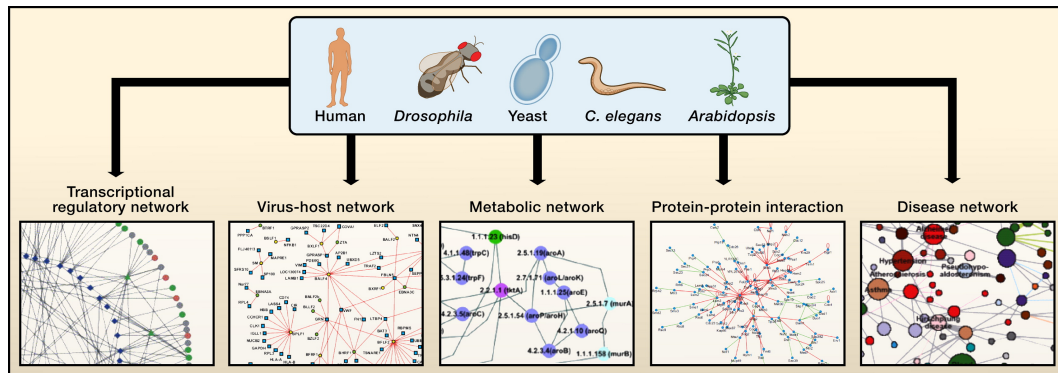


**Figure 6. Networks in cellular systems.** Several types of interactome networks discussed are depicted. In a protein interaction network, nodes represent proteins and edges represent physical interactions. In a transcriptional regulatory network, nodes represent transcription factors (circular nodes) or putative DNA regulatory elements (diamond nodes); and edges represent physical binding between the two. In a disease network, nodes represent diseases, and edges represent gene mutations of which are associated with the linked diseases. In a virus-host network, nodes represent viral proteins (square nodes) or host proteins (round nodes), and edges represent physical interactions between the two. In a metabolic network, nodes represent enzymes, and edges represent metabolites that are products or substrates of the enzymes. The network depictions seem dense, but they represent only small portions of available interactome network maps, which themselves constitute only a few percent of the complete interactome within cells. (Picture adapted from (Vidal et al., 2011)).

## Materials and Methods

### Mice

8-10 weeks old SJL mice were purchased from Charles River Laboratories. The experiments were conducted following the principles of the NIH Guide for the Use and Care of Laboratory Animals and the European Community Council.

### Production of PLP<sub>139-151</sub>-specific encephalitogenic T cell lines

SJL mice were immunized subcutaneously (s.c.) with 300 µg of PLP<sub>139-151</sub> peptide (Genscript, USA) in 200 µl emulsion consisting of equal volumes of phosphate buffered saline (PBS) and CFA (from Difco Laboratories), supplemented with 1 mg/ml of Mycobacterium tuberculosis (strain H37Ra; Difco Laboratories). 10-12 days later, draining lymph nodes were removed and total cells were stimulated with 30 µg/ml of PLP<sub>139-151</sub> peptide for 4 days in culture medium (RPMI 1640 supplemented with 1 mM Na pyruvate, 4 mM GlutaMAX-I® supplement, 100 U/ml penicillin, 100 U/ml streptomycin, 10% v/v fetal bovine serum, and 5 µg/ml plasmocin). PLP<sub>139-151</sub>-specific encephalitogenic T cell lines were obtained by re-stimulation of these cultures every 14 days for at least 3 times in the presence of irradiated splenocytes as antigen presenting cells (APCs) with a proportion of 1:8, and 30 µg/ml of PLP<sub>139-151</sub> peptide.

For our experiments, we considered:

- 1) as actively-proliferating PLP<sub>139-151</sub>-specific encephalitogenic T cells, those collected from lines after 2 days post stimulation (dps);
- 2) as low-proliferating PLP<sub>139-151</sub>-specific encephalitogenic T cells, those cells collected 10-12 dps.

### Pantethine preparation

D-pantethine (pantethine) was purchased from Sigma-Aldrich. For *in vitro* experiments, pantethine was dissolved in PBS to a final concentration of 100 µM and stored at -20°C before use. For *in vivo* experiments, pantethine was dissolved

in physiologic saline solution (0.9% NaCl in water solution) or PBS to a final concentration of 300 mg/ml and stored at -20°C before use.

### **Metabolomics analysis**

Resting CD4<sup>+</sup> T cells were isolated from lymph nodes and spleens of naïve SJL mice by magnetic cell sorting (all reagents from Miltenyi Biotech), whereas actively-proliferating PLP<sub>139-151</sub>-specific encephalitogenic T cells were collected and washed twice with PBS. Cells were pelleted, and cell pellets were immediately frozen in liquid nitrogen and stored at -80°C. In some experiments, actively proliferating encephalitogenic T cells were washed with PBS, re-suspended in fresh medium and treated with PBS or pantethine 1.0 mM for 6 hours before freezing.

Metabolite identification and quantification in T cells were performed in outsourcing by Metabolon (<http://www.metabolon.com/>). Metabolon provided elaborated data via email as Excel data worksheet, including all raw data, average values, ratio values and a variety of statistical evaluations. The subsequent computational studies were performed on metabolites significantly modified between the different sample groups, as determined by Metabolon statistical analysis.

Heatmaps were built using Metaboanalyst 3.0, a comprehensive tool suite for metabolomics data analysis (<http://www.metaboanalyst.ca/>). Pathway, network and metabolism ontology analysis were performed using Cytoscape (Shannon et al., 2003) and the dedicated plugin MetScape (Karnovsky et al., 2012). A global metabolic network was finally constructed from the network output of MetScape, composed by completely connected nodes, representing metabolites, which participate in the identified pathways.

### **Phosphoproteomics and network analysis**

Actively-proliferating PLP<sub>139-151</sub>-specific encephalitogenic T cells were washed twice with PBS, re-suspended in fresh medium and treated with PBS or pantethine 1.0 mM for 6 hours. After treatment, cells were washed and the cell pellet was immediately frozen in liquid nitrogen and stored at -80°C.

Analysis of protein expression and phosphorylation levels was performed in outsourcing by Kinexus (<http://www.kinexus.ca>), using a Kinex™ KAM-850 Antibody Microarray Kit. The Kinex™ Antibody Microarray Service monitored changes in the expression levels and phosphorylation states of signaling proteins with more than 850 antibodies, which includes approximately 517 pan-specific antibodies (for protein expression evaluation) and 337 phospho-site-specific antibodies (for phosphorylation states evaluation). For each antibody, the background-corrected raw intensity data were logarithmically transformed with base 2. Furthermore, Z scores were calculated by subtracting the overall average intensity of all spots within a sample from the raw intensity for each spot, and dividing it by the standard deviations (SD) of all of the measured intensities within each sample (Cheadle et al., 2003). Z ratios were further calculated by taking the difference between the averages of the observed protein Z scores and dividing by the SD of all of the differences for comparisons between actively proliferating PLP<sub>139-151</sub>-specific encephalitogenic T cell treated or not with pantethine. A Z ratio of  $\pm 1.1$  is inferred as significant and used for bioinformatics analysis. Significant proteins were used as a “bioinformatics probe” to build a protein-protein interaction (PPI) network from STRING, a database of known and predicted PPI ([string-db.org](http://string-db.org));(Szklarczyk et al., 2017). The following parameters were set for the analysis: high confidence (0.700) and protein-protein interactions derived only from experiments, text mining and databases.

Network was imported in Cytoscape software for visualization and extraction of a completely connected sub-network. An enrichment analysis with DAVID Bioinformatics Tools for Gene Ontology Biological Process terms and PANTHER signaling pathways (Huang et al., 2009a, 2009b) was performed on protein of the sub-network. Only term with a *P*-value < 0.001 and False Discovery Rate (*FDR*) < 0.05 were considered. Significant terms were organized in a network using Enrichment Map, a Cytoscape plugin, where each term is a node and edges represent protein overlap between terms (Merico et al., 2010).

### ***In vitro* proliferation assays with PLP<sub>139-151</sub>-specific encephalitogenic T cells**

*In vitro* proliferation assays were performed with actively and low proliferating PLP<sub>139-151</sub>-specific encephalitogenic T cells as follow:

- 1) Actively-proliferating PLP<sub>139-151</sub>-specific encephalitogenic T cells were washed twice with PBS, re-suspended in fresh medium and treated with PBS or different concentration of pantethine (0.1 mM, 0.5 mM, 1.0 mM) for 6 hours. Cells were then washed and seeded  $1.0 \times 10^6$ /well in a 96 well plate. 1  $\mu$ Ci/well of [<sup>3</sup>H]-thymidine (<sup>3</sup>H-Tmd; Perkin-Elmer) were added to wells, and cells were left in culture for further 18 hours.
- 2) Low-proliferating PLP<sub>139-151</sub>-specific T cells were washed twice with PBS and incubated for 16 hours with PBS or different concentrations of pantethine (0.1mM and 1.0mM). Cells were then washed and stimulated in 96 well plate. Cells were seeded  $3 \times 10^5$ /well of PLP<sub>139-151</sub>-specific T cells with  $1.2 \times 10^6$ /well of APCs (ratio 1:4) and stimulated with different concentration of PLP<sub>139-151</sub> peptide (10  $\mu$ g/ml, 30  $\mu$ g/ml or nothing). After 6 hours, cells were pulsed with 1  $\mu$ Ci/well of <sup>3</sup>H-Tmd and were left in culture for further 18 hours.

After 18 hours, all samples were then harvested, supplemented with 3 ml of scintillation fluid (Ultima Gold from Perkin-Elmer) and <sup>3</sup>H-Tmd incorporation by proliferating cells was measured with a  $\beta$ -counter (Perkin-Elmer). All experiments were performed in triplicate wells for each condition.

For each experiment, a 96 well plate was seeded for <sup>3</sup>H-Tmd incorporation assay as explained before, and another identical one, but without <sup>3</sup>H-Tmd, for supernatants collection and cell viability assay at the end of the proliferation assay.

### **Bio-Plex assay for cytokines detection**

Supernatants collected from *in vitro* proliferation assays were used for Milliplex cytokine assays (Merck Millipore), following manufacturer's instructions. Briefly, anti-cytokine conjugated beads were plated in 96-well microtiter plates and then removed by vacuum filtration. Samples were then added, and the plate was incubated for 30 min by mixing at 300 rpm. Bio-Plex cytokine assays were sequentially incubated with the detection antibody and

streptavidin-PE; samples were then analyzed immediately by a Bioplex array-system. Unknown cytokine concentrations were automatically calculated by BioPlex software using a standard curve derived from a recombinant cytokine standard. All data were analyzed using PRISM software.

### ***In vitro* adhesion assay on purified integrin ligands**

Twelve-well glass slides were coated for 18h at 4°C with purified mouse Intercellular Cell Adhesion Molecule (ICAM)-1 or Vascular Cell Adhesion Molecule (VCAM)-1 (R&D Systems) 1 µg/ml in PBS, after which were blocked with FBS for 10 minutes at 37°C. PLP<sub>139-151</sub>-specific T cells, collected 8 dps, were pre-treated for 6 hours with increasing concentrations of pantethine (0.1 mM, 0.5 mM, 1.0 mM). Cells were then suspended at 5x10<sup>6</sup>/ml in standard adhesion buffer. 20 µl of cell suspension were added to the wells, and cells were left spontaneously adhere on VCAM-1 or ICAM-1 for 20 min at 37°C. After washing, adherent cells were fixed in glutaraldehyde 1.5% in PBS and counted by computer-assisted enumeration (Bolomini-Vittori et al., 2009).

### **Silencing of CoASY expression in encephalitogenic T cells**

Low-proliferating PLP<sub>139-151</sub>-specific T cells were transfected after 10-13 days from the last *in vitro* antigen-stimulation. Cells were transfected using either 4 µM of specific siRNAs against CoASY or 4 µM of siRNA scrambled as control. Both specific and scrambled siRNAs were purchased as a pool of 4 sequences composed by 19-nucleotides each (ON-TARGET<sup>®</sup> plus siRNA pool from Dharmacon). Transfection was performed with Amaxa's nucleofector technology (Amaxa, Germany) and Mouse T Cell Nucleofector<sup>®</sup> Kit (Lonza) according to the manufacturer's instructions. Briefly, cells were suspended in Nucleofector Solution to a final concentration of 6x10<sup>6</sup> cells/100µl. In Amaxa certified cuvettes, the cells were nucleofected by using the program X-001. Transfected cells were then transferred to 2 ml of pre-warmed medium in 12-wells plate and incubated at 37°C in 7% of CO<sub>2</sub> until use for the proliferation assay as described below. The knockdown efficiency was evaluated by western blot analysis after 24 hours and 48 hours post transfection.



### **CoASY quantification by Western blot analysis**

Cells were lysed for 30 minutes in 1% Nonidet P-40 buffer, containing phosphatase inhibitors and complete protease inhibitor mixture (Roche). Cells lysates were centrifuged at 13000 rpm for 10 minutes at 4°C and Bradford assay (Bio-Rad) was used to estimate protein concentrations. Protein samples were dissolved in sample buffer and boiled for 5 min. Electrophoresis was performed with 7.5% polyacrylamide gels containing 0.1% SDS. Proteins were transferred to nitrocellulose membranes (GE Healthcare) under electrophoretic conditions (400 mA, 1,5 h). Membranes were blocked in Tris-buffered saline with Tween solution (TBST) containing 3% bovine serum albumin (BSA) for 1 h at room temperature (RT). Blots were incubated overnight at 4°C with primary antibodies anti-CoASY (at 1:3000 dilution, ThermoFisher) and anti-β-actin (at 1:3000 dilution, Sigma-Aldrich) in 1% BSA TBST. The following day, blots were rinsed in TBST for 3 times, 10 min each, and incubated for 1 hour at room temperature with appropriate horseradish peroxidase-conjugated secondary antibodies (Amersham Biosciences). Signals were developed using enhanced chemiluminescence (Millipore), and images were captured using ImageQuant LAS 4000 instrument.

Densitometry analysis was performed using Quantity One software (Version 4.6.6, Bio-Rad). The average density is expressed in arbitrary units (Adj volume INT\*mm<sup>2</sup>).

### ***In vitro* proliferation assay with CoASY-silenced PLP<sub>139-151</sub>-specific T cells**

Transfected PLP<sub>139-151</sub>-specific T cells were treated or not with 0.1 mM or 0.2 mM of pantethine for 16 hours within 24 hours after transfection. Cells were then stimulated in 96 well plate with APCs and 30 µg/ml of PLP<sub>139-151</sub> peptide. Subsequent steps of the proliferation assay were performed as described above for low-proliferation PLP<sub>139-151</sub>-specific T cells.

### **Enrichment analysis of a PPI network centered on CoASY using a systems biology approach**

The PPI network of CoASY was built and analyzed using Cytoscape software (Shannon et al., 2003) and dedicated plugins. The “Human Interactome” network (downloaded from “dp.univr.it/~laudanna/LCTST”) was imported in Cytoscape and used as a database network including only experimentally multi-verified protein-protein binary interactions (more information at dp.univr.it/~laudanna/LCTST). A sub-network from the Human Interactome was extracted consisting of CoASY and its directly interacting proteins.

Cytoscape plug-in JEPETTO (Winterhalter et al., 2014) was used to analyze the sub-network centered on CoASY by performing an enrichment analysis of the signaling pathways in which CoASY and its first interacting proteins were involved.

### **EAE induction and *in vivo* treatment with pantethine**

Relapsing-Remitting EAE (RR-EAE) was induced in 8-10 weeks old SJL mice, which were immunized with 300 µg of the PLP<sub>139-151</sub> peptide in 200 µl/mouse of emulsion as described above. Immunization was made with two s.c. injections of 50 µl emulsion in each flank and one of 100 µl in the lower back. 40 ng/mouse of pertussis toxin were injected intravenously at the day of immunization and after 48 hours. To evaluate the clinical benefit of pantethine, mice were treated orally (*per os*, p.o.) with 30 mg/mouse/day of pantethine or with PBS (control animals). In the preventive setting, mice received daily administration of pantethine or corresponding volume of PBS starting 5 days post-immunization. In the therapeutic protocol, pantethine or vehicle was administered p.o after the initial peak of the disease (day +18 post-immunization). In both preventive and therapeutic settings, mice were treated for 20 consecutive days.

Mice were checked for clinical symptoms daily and signs of EAE were translated into clinical score as follows: 0= no disease, 1= tail weakness; 2= paraparesis; 3= paraplegia; 4= paraplegia with forelimb weakness or paralysis; 5= moribund or dead animals.

### **Statistics**

Statistical analyses for metabolomics and phosphoproteomics studies were described above. For the experimental procedures, quantitative data are given as mean values  $\pm$  standard deviation (SD) or standard error of the mean (S.E.M.). Statistical analyses were performed using GraphPad Prism 6 (GraphPad Software Inc., SanDiego, CA). Mann-Whitney U tests were performed to compare groups of unpaired, non-parametric values. Two-tailed paired t tests were used to compare different experimental conditions of paired, parametric values or Wilcoxon tests for paired, nonparametric values. A *P*-value of  $< 0.05$  was considered significant.

## Results

### **Actively proliferating PLP<sub>139-151</sub>-specific T cells display a different metabolic profile compared to resting T lymphocytes**

Myelin-specific encephalitogenic T cells are major players in the development of EAE, the mouse model of human MS (Rangachari and Kuchroo, 2013). In this project, we used these activated encephalitogenic T cells as a model of autoreactive disease-inducing T cells in CNS autoimmunity. We started our study by analyzing the metabolic profile of actively proliferating PLP<sub>139-151</sub>-specific T cells, in comparison with CD4<sup>+</sup> resting T lymphocytes. By performing metabolomics analysis in collaboration with Metabolon (<http://www.metabolon.com/>), we found that encephalitogenic T cells display a metabolic profile very different from resting T cells (**Figure 7**) (Pearce et al., 2013).

***Glycolysis and Krebs cycle.*** Compared to PLP<sub>139-151</sub>-specific T cells, resting T cells showed higher levels of Krebs cycle intermediates, such as CoA, fumarate and malate, suggesting that resting T cells preferentially use OXPHOS for energy production (**Figure 7, Table I**). However, activated encephalitogenic T cells displayed increased levels of free glucose and glycogen-derived molecules, like maltopentaose, maltotetraose and maltotriose, suggesting higher glucose uptake by proliferating T cells (**Figure 7, Table I**). Together with the presence of consistent amount of glycolysis intermediates, like glucose-6-phosphate and fructose-6-phosphate (**Figure 7, Table I**), these data indicate that autoreactive T cells shift their metabolism to aerobic glycolysis during active proliferation. Moreover, the changes in the glycolytic pathways did not account for all metabolic differences between resting and activated encephalitogenic T cells.

***Pentose phosphate pathway (PPP).*** Intermediates of the PPP were also significantly increased in PLP<sub>139-151</sub>-specific T cells, compared to resting T cells (**Figure 7**). Also, PPP, nucleotide, lipid and amino acid building blocks were augmented (**Table I**) suggesting that proliferating T cells actively synthesize macromolecules in an anabolic metabolism necessary for cell growth and replication. Collectively, these data clearly indicate that, as previously reported,

actively proliferating myelin-specific encephalitogenic T cells undergo a metabolic reorganization known as Warburg effect, whereas resting T cells display a metabolic profile typical of resting, non-proliferating cells (Pearce and Pearce, 2013).

**CoA biosynthesis.** Interestingly, our global metabolomics network analysis suggested a downregulation of the CoA synthesis pathway in myelin-specific encephalitogenic T cells compared to resting T cells. In actively proliferating PLP<sub>139-151</sub>-specific T cells, CoA synthesis pathway in the global metabolic network was characterized by a decrease in the pantothenate uptake, followed by an accumulation of 3'-dephospho-CoA and lower levels of free CoA (CoA-SH) (**Figure 7, Table I**).

### **CoA fueling inhibits anabolic metabolism in PLP<sub>139-151</sub>-specific effector T cells**

Considering the downregulation of CoA synthesis pathway in actively proliferating encephalitogenic T cells compared to resting T cells, we hypothesized that CoA fueling could potentially alter the metabolic profile interfering with pathogenic functions of autoreactive T cells. To investigate such possibility, we used the low molecular weight thiol pantethine, the stable homodimeric form of pantotheine, which represents the metabolic precursor of CoA molecule (**Figure 8**). Pantethine was previously shown to increase CoA levels both in vitro and in vivo (Branca et al., 1984a; Rana et al., 2010).

We firstly evaluated the whole impact of CoA fueling on PLP<sub>139-151</sub>-specific encephalitogenic T cell metabolic pathways by performing metabolomics analysis on pantethine-treated PLP<sub>139-151</sub>-specific T cells. We observed that 6h treatment of these cells with pantethine induced a consistent alteration in the intracellular content of at least 158 metabolites (**Table I**).

By performing network analysis using a systems biology approach, all metabolites modified by the pantethine treatment were organized in a global metabolomics network. Overall, the network obtained allowed us to propose a model on the global mechanism of action of pantethine in T cells, which is described below.

***Glycolysis and Krebs cycle.*** The broad effect of CoA fueling affected the glycolysis pathway and reduced glucose uptake, as suggested by the 1.4-fold reduction of free glucose concentration (**Figure 9, Table I**). Moreover, the consistent reduction of glucose-6-phosphate, its precursor, mannose-6-phosphate, and other glycolysis metabolites such as fructose-6-phosphate and fructose 1,6-diphosphate, confirmed our observations suggesting an inhibition in the glycolytic pathway induced by pantethine (**Figure 9, Table I**).

***PPP.*** Importantly, the reduced availability of fructose 6-phosphate and fructose 1,6-diphosphate, which link glycolysis to the PPP, was accompanied by the reduction of metabolites arising from the non-oxidative phase of PPP, such as ribulose 5-phosphate (isobar with xylulose-5-phosphate), ribose 5-phosphate and sedoheptulose-7-phosphate (**Figure 9, Table I**). The block of PPP was also confirmed by an increase in the amount of the metabolite linking oxidative to non-oxidative PPP phases: the 6-phosphogluconate (Sukhatme and Chan, 2012) (**Figure 9, Table I**).

***FAO.*** Beyond glycolysis, resting and proliferating T cells differ in their use of FAO pathway for energy supply (MacIver et al., 2013). The changes in lipid metabolism observed after pantethine treatment were mainly correlated with an induction of membrane remodeling. In particular, pantethine increased the amount of the phospholipid precursor cytidine-5'-diphosphocholine and the major degradation product of choline-containing phospholipids: the glycerophosphorylcholine (GPC) (**Figure 9, Table I**). Interestingly, the increase in GPC content may be related to an increased synthesis of phosphatidylcholine (Baburina and Jackowski, 1999), which is a potent activator of both enzymatic activities of CoASY *in vitro* (Zhyvoloup et al., 2003). In accordance, the increase in phosphatidylcholine is correlated with a reduction in 3'-dephospho-CoA after pantethine treatment in favor of an increased CoA synthesis and a consequent limitation of phospholipids availability due to the membranes assembling during proliferation. Moreover, we also found a reduction of 1-palmitoylglycerophosphoethanolamine, suggesting a shift to FAS or an acceleration of FAO, leading to accumulation of glycerol phospholipids-containing shorter chain fatty acids (**Figure 9, Table I**).

***Purine and pyrimidine metabolism.*** In proliferating cells, shift to aerobic glycolysis induced an anabolic metabolism essential for the synthesis of protein and nucleic acid building blocks necessary for cell growth and division (Vander Heiden et al., 2009). Our metabolomics analysis confirms a reduction of such pathways in encephalitogenic T cells after pantethine treatment. Indeed, we observed that several intermediates and end products of the purine and pyrimidine synthesis pathways were variably reduced by pantethine treatment, such as adenosine-3'-monophosphate (3'-AMP), adenosine-5'-diphosphoribose, 2'-deoxyadenosine-3'-monophosphate, 2'-deoxyguanosine, 2'-deoxyinosine, xanthine, orotate and N-carbamoylaspartate (**Figure 9, Table I**), suggesting that pantethine, together with the inhibition of PPP, likely affected DNA and RNA synthesis.

***Amino acids metabolism.*** Interestingly, the CoA fueling also impacted the metabolism of several amino acids, and, in particular, we observed a reduction in the levels of many free amino acids and correlated elevations in some dipeptides (**Figure 9, Table I**). These changes may be indicative of increased protein degradation/turnover due to changes in gene expression programs and/or greater use of amino acids to meet energy demands as a source of carbons.

***Glutathione metabolism and oxidative stress.*** Overall, our data suggest an increase of the catabolic metabolism boosted by CoA fueling (with amino acids, fatty acids and carbohydrate as sources), possibly resulting in a general increase of OXPHOS. As highly oxidative processes, such as FAO and OXPHOS, may be associated with huge ROS production, the general increase in the catabolic metabolism after CoA fueling may cause intracellular oxidative stress. Glutathione is the most important intracellular antioxidant and serves as a redox buffer cycling between its reduced and oxidized (GSSG) forms, and thus the ratio between GSH and GSSG serves as an indicator of intracellular oxidative stress. We found that pantethine treatment increased the total glutathione levels in PLP<sub>139-151</sub>-specific encephalitogenic T cells (**Figure 9, Table I**). Although this aspect may suggest an antioxidant effect of pantethine, as previously demonstrated (Cornille et al., 2010), we observed a decrease in the ratio GSH/GSSG, which is an index of an increase in the intracellular oxidative stress

and ROS levels, probably due to an augmented oxidative metabolism. Interestingly, recent studies demonstrated that glutathione and ROS play a key role in the regulation of T cell proliferation, growth, and function (Nathan and Cunningham-Bussel, 2013). In particular, high level of intracellular ROS was demonstrated to inhibit mTOR pathway and the metabolic reprogramming of activated T cells (Mak et al., 2017). In addition, S-adenosylhomocysteine (SAH), a precursor for glutathione synthesis, and levels of 5-oxoproline, an intermediate produced when glutathione is degraded and recycled via the  $\gamma$ -glutamyl cycle, were also higher in autoreactive T cells (**Figure 9, Table I**). Taken together, these metabolic changes may confirm increased glutathione synthesis (Cornille et al., 2010). As cysteine is required for CoA synthesis and is the rate-limiting biochemical molecule for glutathione synthesis, pantethine treatment and modulation of CoA metabolism could potentially contribute to the observed changes in glutathione metabolism.

**CoA biosynthesis.** As expected, treatment with pantethine was associated with changes in CoA biosynthesis pathway, as suggested by the significant elevation (about 34-fold increase) in pantothenate, the primary precursor for CoA synthesis. Moreover, intracellular levels of the CoA precursor 3'dephospho-CoA were significantly reduced after pantethine treatment (**Figure 9, Table I**). Overall, the increase in pantothenate uptake and reduction in 3'dephospho-CoA level suggested a restoration of CoA synthesis pathway in myelin-specific T cells, which were reprogrammed towards a resting-like state. Unexpectedly, metabolomics analysis showed a reduction in free CoA level in pantethine treated cells after 6 hours of treatment. We hypothesize that the decreased level of CoA-SH is due to higher consumption of CoA-SH in the numerous reactions in which this molecule is involved. In light of these data, we decided to further investigate the intracellular levels of CoA in pantethine treated myelin-specific encephalitogenic T cells by performing fluorometric *in vitro* assays (CoA Colorimetric/Fluorometric Assay Kit, Biovision). Unfortunately, results were not reproducible due to limited detection sensitivity of the kit. However, our data suggest that treatment of encephalitogenic T cells with pantethine led to rapid consumption and modulation of CoA metabolism, rather than a real increase in



the amount of CoA-SH (data not shown). In accordance with metabolomics data showing a decrease in CoA-SH level, we observed an increase in acyl-CoA molecules, suggesting that free CoA derived from a potentiated CoA synthesis pathway is rapidly metabolized in the numerous metabolic pathways, in which CoA is involved. Nevertheless, the data obtained by fluorometric analysis need to be confirmed by performing a more sensitive assay such as HPLC-MS (high performance liquid chromatography-mass spectrometry).

### **Phosphoproteomics analysis elucidated the immuno-modulatory effect of CoA fueling in PLP<sub>139-151</sub>-specific T cells**

As CoA fueling with pantethine highly impacted the intracellular metabolic profile of encephalitogenic T cells, which shifted toward a resting-like state, we hypothesized that such metabolic reprogramming may have an immuno-modulatory effect on PLP<sub>139-151</sub>-specific autoreactive T cells. To investigate the net effect of CoA fueling on encephalitogenic T cell functions, we performed phosphoproteomics analysis on actively proliferating PLP<sub>139-151</sub>-specific effector T cells treated or not with pantethine. 234 significant proteins were selected as bioinformatics probe components with a Z-ratio of  $\pm 1.1$  in terms of expression or phosphorylation differences between encephalitogenic T cells treated or not with pantethine (**Table II**). We used this probe to generate a protein-protein interaction network from the STRING database (Szklarczyk et al., 2017). The network was imported in Cytoscape and an entirely connected sub-network with 204 nodes was obtained. Gene Ontology Biological Process (GOBP) terms and PANTHER pathways enrichment analysis was performed on the 204 nodes with DAVID Bioinformatic tool (Huang et al., 2009a, 2009b), and  $P$ -value $<0.001$  and False Discovery Rate (FDR) $<0.05$  were set as thresholds. Terms were finally organized in two networks using Enrichment Map plugin on Cytoscape: a network of 117 nodes was obtained for the GOBP enrichment analysis and a network of 24 nodes was obtained for PANTHER pathways (**Figure 10**). The bioinformatics analysis revealed that the majority of GO term referred to general biological processes related to intracellular signaling cascade, homeostatic processes, apoptosis, and immune-related biological processes such as cell proliferation, cell migration,

cytokine-mediated pathway, and Jak-Stat cascade (**Figure 10**). In addition, PANTHER pathways enrichment analysis revealed specific signaling pathways modified by pantethine treatment, related to GO biological processes identified, such as T cell activation, Ras, Jak/Stat, P38 Mapk, PI3 Kinase, integrin, toll receptor and cytokine-mediated pathways such as interferon-gamma and other interleukins (**Figure 10**). Collectively, data from this high throughput analysis suggest that CoA fueling has a strong immuno-modulatory effect on PLP<sub>139-151</sub>-specific encephalitogenic T cells and may significantly affect their metabolism, activation, proliferation and pathogenic features.

### **CoA fueling has immuno-modulatory effects on PLP<sub>139-151</sub>-specific T cells**

Data obtained by phosphoproteomics computational analysis suggested an effect of CoA fueling on intracellular signaling pathway related to the immune response, in particular, **cell proliferation, cell adhesion and cytokine production**. In light of these results, we next investigated the possible immuno-modulatory effect of CoA fueling on the pathogenic features of encephalitogenic T cells.

*Pantethine treatment inhibits proliferation of T cells in vitro.* We firstly analyzed the effect of pantethine on the antigen-induced proliferation of PLP<sub>139-151</sub>-specific encephalitogenic T cells. We found that 6 h treatment with pantethine of actively-proliferating encephalitogenic T cells significantly reduced their proliferative capacity in a dose-dependent manner (**Figure 11**). The inhibition of pantethine on the proliferative capacity of actively-proliferating encephalitogenic T cells suggested that CoA fueling affects the active inflammation process, by reducing metabolic pathways and, consequently, signaling pathways essential for active proliferation.

To evaluate the potential of preventive CoA fueling on T cell activation, we then tested the capacity of CoA potentiation to inhibit antigen-stimulation and activation of encephalitogenic T cells. We found that 16 hours pre-treatment with pantethine strongly inhibited antigen-specific T cell proliferation in a dose-dependent manner (**Figure 12**). These data confirm that pantethine affects the

proliferation of pathogenic effector T cells, by limiting their re-stimulation by APCs *in vitro*.

***Pantethine treatment reduces pro-inflammatory cytokine production of T cells in vitro.*** Several pro-inflammatory cytokines produced by pathogenic T cells were identified to play a key role in both EAE and human MS development (Petermann and Korn, 2011). For this reason, we investigated the effect of pantethine pre-treatment on cytokine production by encephalitogenic T cells quantifying cytokine amounts in supernatants from proliferation assays. We found that the reduced T cell proliferation was accompanied by a strongly reduced pro-inflammatory cytokine production by pantethine-treated T cells (**Figure 13**). In particular, pantethine reduced the production by encephalitogenic T cells of IL-6, IL-17, IFN- $\gamma$ , granulocyte macrophage colony-stimulating factor (GM-CSF) and TNF- $\alpha$ , which were shown to be essential for EAE development (Petermann and Korn, 2011) (**Figure 13**), confirming that pantethine blocks T cell activation *in vitro*.

***Pantethine treatment inhibits spontaneous T cell adhesion in vitro.*** The ability of encephalitogenic T cells to adhere on inflamed CNS pial venules and to migrate in the surrounding CNS parenchyma is a crucial event in the induction of inflammatory responses against neuronal myelin sheath (Piccio et al., 2002; Rangachari and Kuchroo, 2013; Rossi et al., 2011). It was previously shown that pantethine treatment down-regulates platelet hyper-adhesion in an animal model of cerebral malaria, suggesting that pantethine may impact cell adhesion to activated endothelium (Penet et al., 2008). Pantethine was also recently shown to affect resting T cells adhesion *in vitro* (van Gijssel-Bonnello et al., 2015). In order to test whether CoA fueling may modulate the adhesive capacity of autoreactive T cells, we investigated the effect of pantethine treatment on the integrin-dependent adhesion of encephalitogenic T cell on purified ICAM-1 and VCAM-1 *in vitro*. We found that pre-treatment with pantethine significantly reduced the spontaneous adhesion of encephalitogenic T cells on both integrin ligands in a dose-dependent manner when compared to untreated cells (**Figure 14**). These data suggest that pantethine can inhibit activated T cell adhesiveness by modulating integrin activation on autoreactive T cells.

### **Silencing of CoASY abolished pantethine inhibitory effect in PLP<sub>139-151</sub>-specific T CoA fueling**

CoASY is the enzyme that catalyzes the last two sequential steps of CoA synthesis, which represent a critical point for CoA production. In order to confirm that the metabolic reprogramming induced by pantethine in encephalitogenic T cells was due to CoA fueling, we performed proliferation assays after CoASY silencing in PLP<sub>139-151</sub>-specific T cells.

PLP<sub>139-151</sub>-specific T cells were transfected with siRNA-CoASY using electroporation as described in methods. Post transfection western blot analysis confirmed 50% reduction in CoASY expression after 24h silencing, whereas 48h silencing was not effective (**Figure 15**).

Therefore, within 24 hours post transfection we performed proliferation assays with siRNA-CoASY transfected PLP<sub>139-151</sub>-specific T cells, analyzing the impact of pantethine treatment on their proliferative capacity. Scramble siRNA-transfected cells were used as control condition. The results showed a significant reduction of the inhibitory effect of pantethine treatment on the proliferation rate of siRNA-CoASY transfected PLP<sub>139-151</sub>-specific T cells, whereas control siRNA-scramble transfected PLP<sub>139-151</sub>-specific T cells were inhibited in their proliferative capacity by pantethine (**Figure 16A**). These data confirm that the inhibitory effect of pantethine on T cell proliferation was due to de novo CoA synthesis in treated cells. Interestingly, the proliferation assays showed that, in absence of pantethine treatment, siRNA-CoASY transfected PLP<sub>139-151</sub>-specific T cells displayed an increased basal proliferation even in the absence of antigenic stimulation, compared to siRNA-scramble transfected T cells (**Figure 16B**), suggesting that CoA synthesis pathway can be modulated to regulate T cell activation and functions.

### **CoASY– RPS6KB1 complex links cellular metabolism to immune related signaling pathways**

Considering the results obtained from silencing experiments showing that the knockdown of CoASY in activated, but low-proliferating, encephalitogenic T

cells acted as a sort of activation input, we next studied the role of CoASY as a potential direct link between metabolic reprogramming and the pathogenic features of antigen-specific T cells. Previous studies on immunometabolism have demonstrated that metabolic enzymes have secondary tasks, distinct from their classical role (such as RNA binding and pathogen recognition), controlling many different aspects of immune cell activation, fate and function. Examples of such enzymes are glyceraldehyde 3-phosphate dehydrogenase (GAPDH), pyruvate kinase (PK), and hexokinase (HK) (Chang et al., 2013; Palsson-McDermott et al., 2015; Wolf et al., 2016). Moreover, recent studies have showed that CoASY forms complexes with intracellular signaling proteins involved in the immune response, such as p85 $\alpha$  regulatory subunit of PI3K (Breus et al., 2009), tyrosine phosphatase Shp2PTP, tyrosine kinase Src (Breus et al., 2010), ECD4 (Gudkova et al., 2012) and RPS6K1 (Nemazanyy et al., 2004). This aspect was confirmed by our preliminary analysis with a systems biology approach on a PPI network built around CoASY. Indeed, in the bioinformatics analysis, RPS6KB1 resulted as the most important linker protein between CoASY and immune related signaling pathways. The data suggested that the direct interaction between CoASY and RPS6KB1 may have a role in the regulation of signaling pathways related to cell proliferation, cytokine production and cell motility through effects on Mapk, Rac1 and mTOR pathways (**Figure 17**). The physical interaction between CoASY and RPS6KB1 has been demonstrated in HEK293 and MCF7 cell lines (Nemazanyy et al., 2004). In this study Nemazanyy et al. uncovered a potential link between mTOR/S6K signaling pathway and energy metabolism through CoA and its thioester derivatives, but its physiological relevance needs to be further elucidated.

Our hypothesis is that CoASY could be modulated during differentiation of encephalitogenic T cells and that pantethine treatment may potentiate CoASY activity, influencing its expression, phosphorylation level and formation of complexes with intracellular proteins, such as RPS6KB1.

**Pantethine inhibits EAE development and ameliorates clinical outcome in established EAE**

Recent data showed that administration of pantethine had beneficial effects in several animal models of neuroinflammation and neurodegeneration, such as cerebral malaria, Pank-associate neurodegeneration and Parkinson disease (Brunetti et al., 2014; Cornille et al., 2010; Penet et al., 2008; Rana et al., 2010). In light of the dramatic metabolic and immuno-modulatory properties of CoA fueling by pantethine treatment on PLP<sub>139-151</sub>-specific effector T cells *in vitro*, we evaluated immunomodulation by pantethine *in vivo* on the pathogenesis of EAE. We found that preventive treatment with pantethine reduced the incidence and strongly affected the severity of RR-EAE in SJL mice, with a drastic reduction of maximal clinical score as well as cumulative score compared to control animals (**Figure 18, Table III**). Importantly, the protective effect of pantethine was maintained even after the suspension of the treatment (**Figure 18**).

Considering the potential translational impact of pantethine in humans, we next tested pantethine in a therapeutic setting, by treating SJL after the initial peak of disease. We found that therapeutic pantethine administration significantly ameliorated disease severity in RR-EAE, with reduced relapses and significantly lower cumulative score and mean maximum score after the beginning of the treatment (**Figure 19, Table IV**). These results demonstrated that pantethine treatment and CoA fueling has not only a protective effect on autoimmune disease development, but can also interfere with established disease mechanisms and ameliorates autoimmune disease progression.

## Discussion

A continuous increase in the incidence of autoimmune diseases is to be expected in the aging societies worldwide. Autoimmune disorders not only cause severe disability and chronic pain, but also lead to considerable socio-economic costs. Given that the current treatment options are not curative, have substantial side effects and a significant percentage of patient are non-responders, innovative therapeutics for the treatment of autoimmune pathologies are needed.

In recent years, it has become clear that metabolism critically influences the outcome of an immune response and that generation and activation state of different T cell subsets are controlled by the preferential engagement of distinct metabolic pathways (Lochner et al., 2015; O'Sullivan and Pearce, 2015). Growing evidence suggest that changes in the metabolism of immune cells are associated with their effector functions and contribute to the pathogenesis of autoimmunity. Additionally, although they affect different target organs, some autoimmune diseases share alterations in metabolic pathways, key metabolites or metabolic by-products such as modifications in amino acid, ROS, cholesterol levels or glucose catabolism. Thus, the emerging field of immunometabolism may lead to the discovery of novel therapeutic targets for the treatment of multiple diseases. In this study, by using metabolomics, proteomics and functional approaches, we demonstrated that CoA synthesis pathway have a role in the regulation of the activation and the effector functions of autoreactive T cells, in particular myelin-specific encephalitogenic T cells, which represent the major players in the pathogenesis of EAE, the animal model of MS.

In agreement with previous literature, our metabolomics analysis clearly demonstrated that myelin-specific encephalitogenic T cells shift their metabolism to aerobic glycolysis and anabolic metabolism when activated by antigen presentation. This metabolic change is known as “Warburg effect” and it is characterized by an increase in free fatty acids levels and several metabolites related to glycolysis, Krebs cycle and PPP, in immune cells in response to activating stimuli (Gerriets and Rathmell, 2012; MacIver et al., 2013; Pearce and Pearce, 2013; Pearce et al., 2013; Vander Heiden et al., 2009). Interestingly, we

also observed a reduced intracellular CoA synthesis correlated with a reduction in the uptake of pantothenate, which is the first metabolite of the CoA synthesis pathway, and an accumulation of 3'-dephospho-CoA, the direct precursor of CoA metabolized by the enzyme CoASY (Sibon and Strauss, 2016). Previous reports suggested a therapeutic potential for aerobic glycolysis inhibition in autoimmune disease development (Bian et al., 2009; Gerriets et al., 2015; Shi et al., 2011), but the modulation of CoA synthesis as a new therapeutic target for the treatment of inflammatory and autoimmune pathologies was never investigated so far. Therefore, in the present study we investigated the immuno-modulatory effect of metabolic treatment with the low molecular weight thiol pantethine, a CoA precursor, on autoreactive T cell activation and EAE development (Branca et al., 1984a; Cighetti et al., 1987; Rana et al., 2010).

CoA is an indispensable metabolite for mammalian cells, as it is involved in more than 100 different biochemical reactions and about 4% of known enzymes use it as a cofactor (Leonardi et al., 2005). In this study we have shown that CoA fueling with pantethine induced a broad metabolic re-organization in proliferating autoreactive T cells, reprogramming them to a "resting-like state" characterized by reduced glycolytic rates, inhibition of PPP pathway and nucleic acid synthesis and reorganization of the lipid and protein content in treated cells. We thus hypothesized that metabolic reprogramming by pantethine may have an immuno-modulatory effect on PLP<sub>139-151</sub>-specific autoreactive T cells. To further investigate the effect of CoA fueling on encephalitogenic T cell functions we performed a phosphoproteomics analysis, using a high throughput antibody microarray approach to evaluate the impact of pantethine on protein expression and phosphorylation levels in encephalitogenic T cells. Although many post-transcriptional protein modifications are involved in intracellular signaling, phosphorylation of serine, threonine and tyrosine residues is the one most commonly used signaling mechanism in mammalian cells (Caenepeel et al., 2004; Manning et al., 2002). In the current study, we identify 234 proteins significantly modified by pantethine treatment in terms of phosphorylation and/or expression levels. The complex bioinformatics analysis we performed revealed that pantethine is able to affect crucial immune processes associated with the



functionality and the pathogenicity of encephalitogenic T cells, such as cell activation and proliferation, cytokine production, cell adhesion and migration. To note, the PPI network obtained from our bioinformatics analysis using a systems biology approach will be useful for future investigation to identify signaling pathways and specific targets affected by pantethine treatment. Importantly, in accordance with data from metabolomics and phosphoproteomics analysis, we experimentally confirmed that CoA fueling strongly affected the pathogenic features of PLP<sub>139-151</sub>-specific encephalitogenic T cells, by reducing their proliferative capacity and pro-inflammatory cytokine production following antigenic stimulation and their integrin-dependent adhesion *in vitro*. These results clearly indicate that our bioinformatics approach efficiently identified the key immune-related processes modified in encephalitogenic T cells, which return to a resting-like state after CoA fueling with pantethine.

The capacity of CoA fueling to reduce the activation and cytokine production *in vitro* in encephalitogenic T cells by reducing the glycolytic rate is in accordance with a previous report showing that engagement of aerobic glycolysis by activating T cells is crucial for their effector functions (Chang et al., 2013). However, Chang and colleagues demonstrated that this metabolic shift is not required for T cell proliferative capacity (Chang et al., 2013), whereas we demonstrated that pantethine treatment also reduced T cell proliferation. This result suggests that pantethine influences more metabolic or signaling pathways other than, or in addition to, its ability to reduce aerobic glycolysis. A possible explanation is the ability of pantethine to influence lipid plasma membrane in treated cells, by decreasing lipid rafts formation as previously reported (van Gijzel-Bonnello et al., 2015). Activation of T cells through the TCR is indeed dependent on its localization in cholesterol-rich lipid membrane rafts, which are essential for trans-membrane signaling (Horejsi and Hrdinka, 2014). Our preliminary results (not shown) confirm that pantethine, due to its ability to affect lipid synthesis and increase FAO, dissolved pre-formed lipid rafts in activated T cells, and potentially dislocate essential signaling proteins from the immunological synapse *via* modification of plasma membrane composition. Moreover, the capacity of CoA fueling to reduce integrin-dependent cell adhesion

may be related to the influence on integrin functionality, which may also depend on their localization into cholesterol-rich membrane lipid rafts on cell surface (Korade and Kenworthy, 2008). In this context, it has been previously demonstrated that cholesterol depletion inhibits adhesion on VCAM-1 and ICAM-1 of activated T cells (Leitinger and Hogg, 2002). Thus, our data suggest that CoA fueling broadly impacts autoreactive T cell activation, beyond its ability to affect Warburg effect by a decrease in the glycolytic rate.

To confirm that the metabolic reprogramming of encephalitogenic T cells induced by pantethine was indeed due CoA fueling, we performed a siRNA-mediated silencing of CoASY in encephalitogenic T cells. CoASY is the enzyme that catalyzes the last two sequential steps of the CoA synthesis pathway, which represents the only way for *de novo* CoA production in the cell (Sibon and Strauss, 2016). Proliferation assays showed that siRNA-CoASY-transfected encephalitogenic T cells were no more sensitive to pantethine treatment after antigenic stimulation, compared to scrambled siRNA-transfected cells, confirming that pantethine play its immuno-modulatory through an increase CoA synthesis. Interestingly, proliferation experiments also showed that the knockdown of CoASY acted as an activation input in low-proliferating encephalitogenic T cell. Indeed, in the absence of antigen stimulation, siRNA-CoASY transfected encephalitogenic T cells increased their basal proliferative capacity, indicating a key role for CoA synthesis in the control of autoreactive T cell activation and function. Based on our results, we also speculate the CoASY may act as a link between metabolic reprogramming and the pathogenic features of antigen-specific T cells. Indeed, it was recently reported that several metabolic enzymes might also have secondary tasks in the cytoplasm distinct from their classical role. Metabolic enzymes could modulate cellular processes such as RNA binding and pathogen recognition, which are essential for immune cell including activation, polarization and function. GAPDH, PK, and HK, are examples of enzyme which moonlighting functions, acting as RNA binding and pathogen recognition proteins, beyond their role enzymatic activity (Chang et al., 2013; Palsson-McDermott et al., 2015; Wolf et al., 2016). CoASY represents an essential regulator of cell energy metabolism due to its role in the production of CoA, but recent studies have also shown that

CoASY is able to form complexes with intracellular signaling protein involved in the immune response, such as RPS6KB1 (Nemazanyy et al., 2004). Interestingly, from our bioinformatics analysis on CoASY-centered PPI network, RPS6KB1 resulted as the most important link protein between CoASY and immune related signaling pathways such as Mapk, Rac1 and mTOR pathways. CoASY may create a complex with RPS6KB1 through the interaction of their C-terminal region, in which CoASY has its catalytic domain necessary for CoA production. The formation of the complex could be one mechanism of regulation of downstream signaling pathways through a modulation of CoA production and *vice versa*. Based on that, our future goal will be to further investigate the role of CoASY-RPS6KB1 complex in immune responses, in particular on the effector functions of autoreactive T cell and autoimmunity. Our hypothesis is that CoASY could be modulated during differentiation of encephalitogenic T cells and that pantethine treatment, by inducing potentiation of CoASY activity through CoA fueling, could influence the expression, phosphorylation level and formation of complexes with intracellular proteins, including RPS6KB1. To note, transcriptomics data on the GEO database ([www.ncbi.nlm.nih.gov/gds](http://www.ncbi.nlm.nih.gov/gds)) suggest that that CoASY is downregulated in the first hours (from 2 to 6 hours) of CD4<sup>+</sup> T cell antigen-stimulation. The later observation, in accordance with the increase in the proliferation rate of unstimulated PLP<sub>139-151</sub>-specific T cells after CoASY silencing, suggests that the transient downregulation of CoASY may trigger early T cell activation. This observation opens new opportunities for further studies on the role of CoASY in the control of autoreactive T cell activation and functions in autoimmune diseases, and CoASY agonists/antagonists may be developed to finely tune the metabolism and signaling pathways of autoreactive immune cells.

The strong immuno-modulatory effect of pantethine on encephalitogenic T cells, together with recent data suggesting a potential therapeutic application of pantethine in CNS inflammatory diseases (Cornille et al., 2010; Penet et al., 2008; Rana et al., 2010), prompted us to investigate the impact of such immunomodulation *in vivo*, on the development of EAE, the animal model of MS. Our data indicated that preventive treatment with pantethine, during the preclinical phase, inhibited the development of EAE in PLP<sub>139-151</sub>-immunized

mice, suggesting that CoA fueling interferes with immune processes essential for disease onset. Most importantly, considering a possible therapeutic use for pantethine in human MS patients, therapeutic administration of pantethine after the first disease peak in mice with established EAE, strongly reduced the disease severity, suggesting that pantethine is also able to interfere with disease-associated processes that lead to further worsening of the pathology. In other animal models of neurological diseases, pantethine was previously shown to have protective effects thanks to its antioxidant properties and ability to increase mitochondrial functions in damaged neurons (Brunetti et al., 2014; Cornille et al., 2010; Rana et al., 2010). Our data showed that pantethine impacted glutathione metabolism in encephalitogenic T cells, suggesting that pantethine treatment may potentially have antioxidant effect and may induce neuroprotection in EAE mice. Moreover, in a mouse model of cerebral malaria, Penet and colleagues demonstrated a protective role for pantethine on BBB leakage (Penet et al., 2008), and these data are in agreement with our preliminary data showing a reduced BBB leakage in pantethine-treated EAE mice (data not shown). Thus, pantethine may not only reduce immune cell activation, but may have a broader protective impact *in vivo* in EAE mice.

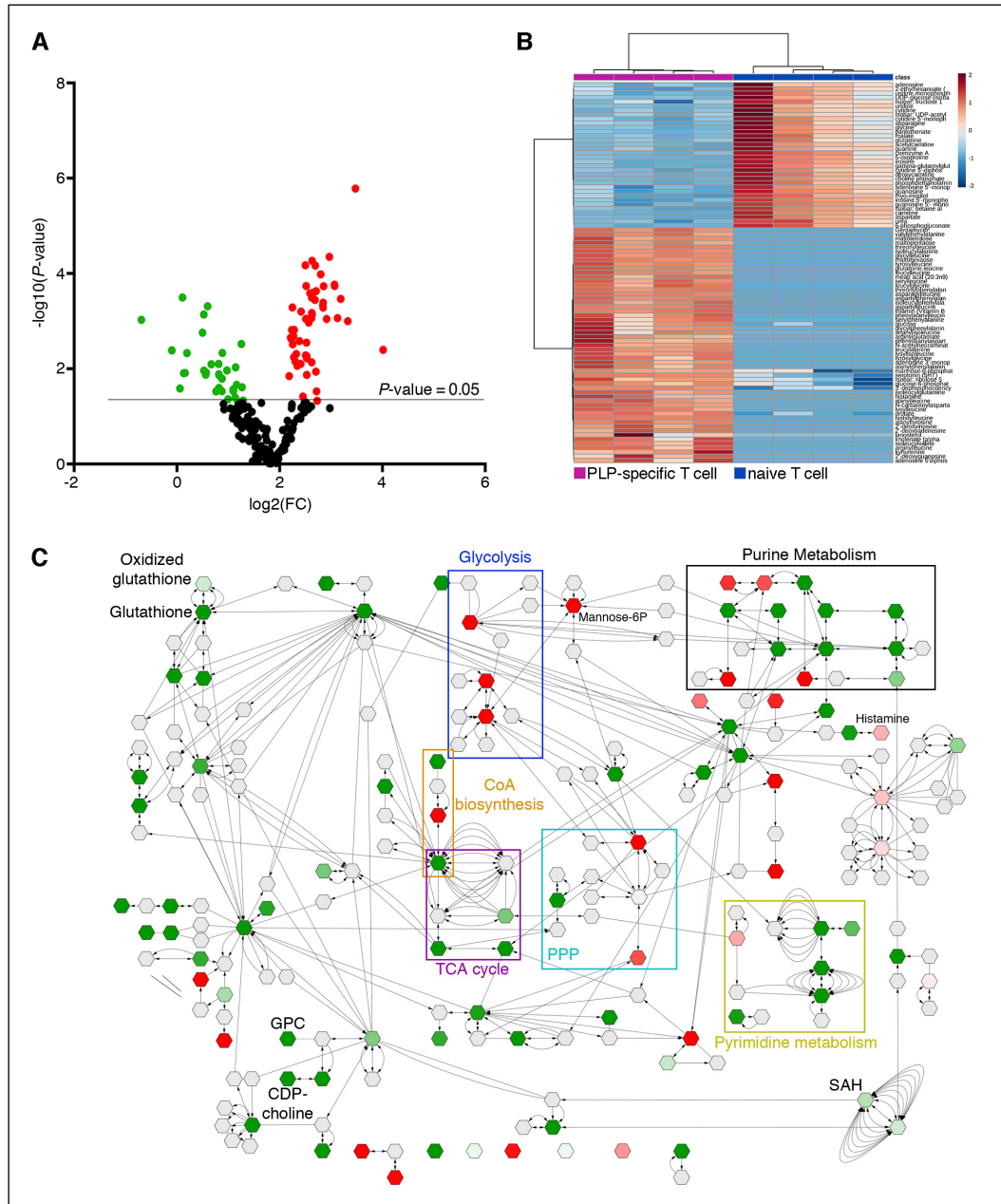
The use of pantethine to treat autoimmune and inflammatory pathologies may be rapidly translated to humans, as pantethine is used from early '70s as a lipid-lowering drug in hyperlipidemic patients, with any important side effects reported (Evans et al., 2014; Horváth and Vécsei, 2009; Rumberger et al., 2011). To note, as pantethine is administered orally in humans, mice were also treated *per os* by gavage in our study. One of the main drawbacks of the current MS therapy is the route administration, with the majority of drugs requiring intravenous, intramuscular or sub-cutaneous injections. Moreover, current therapies are still only partially effective and have high costs and risk of severe side effects, limiting their use for the treatment of the human disease (Wingerchuk and Carter, 2014). Therefore, oral pantethine-based therapy in human MS may ameliorate the lifestyle of MS patients, avoiding the invasive administration routes of current therapeutic approaches.

As previously reported in other models (Cornille et al., 2010; Penet et al., 2008), we observed that pantethine derivatives such as pantothenic acid (vitamin B5), cystamine and cysteamine did not display any beneficial effect *in vivo* in EAE mice (data not shown), suggesting that the entire pantethine molecule is necessary for an efficient immuno-modulation of the inflammatory response. Previous studies indicated that pantethine undergoes rapid hydrolysis in the small intestine, with rapid absorbance at this level (Wittwer et al., 1985), suggesting an effective use of this drug as a precursor of CoA in the liver (Branca et al., 1984b). Although this therapy has therapeutic potential, several limitations may exist, including incomplete data regarding bioavailability, pharmacokinetics, and ability of this compound to cross the BBB. In collaboration with a pharmaceutical company, we recently developed two novel molecular formulations of pantethine to increase the bioavailability and efficacy in the treatment of EAE (data not shown). The first formulation was designed to protect the molecule from gastric acidity and increase absorption in the first part of the intestine, whereas the second one was designed to release pantethine immediately in the stomach. We obtained very preliminary data showing that the first formulation is very efficient in the treatment of EAE (data not shown), paving the way for the potential therapeutic use of new pantethine formulations in autoimmune and inflammatory pathologies.

Overall, the results obtained in our study suggest a crucial role for the CoA synthesis pathway in the control of autoreactive T cell activation and autoimmune disease development. Also, further studies will help to understand the role of CoASY in metabolic and protein-protein interaction networks during T cell activation, opening new avenues for the development of novel therapeutic approaches to finely modulate T cell activation and autoimmunity.

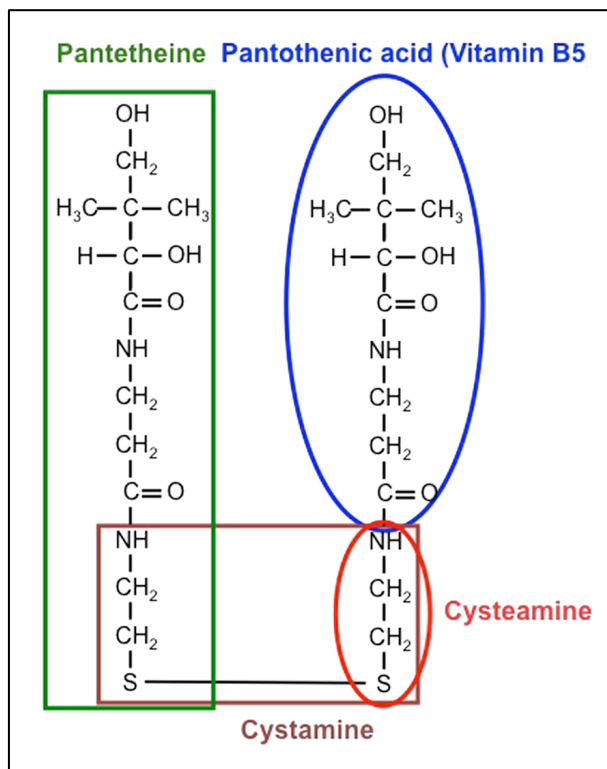
# Figures and Tables

Figures 1-6 are shown in the Introduction.



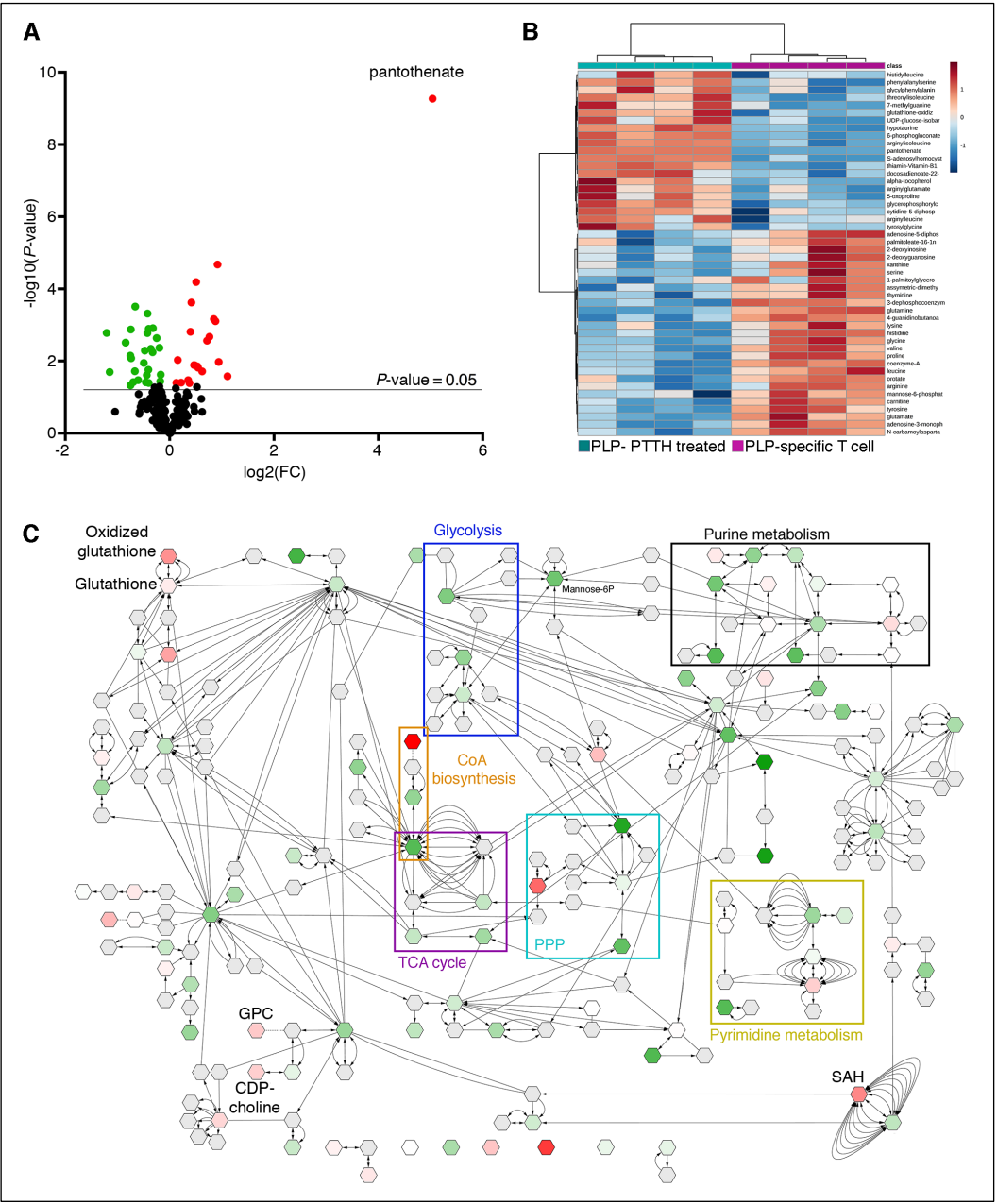
**Figure 7. Metabolomics analysis uncovered the metabolic reprogramming of actively-proliferating encephalitogenic T cells.** CD4<sup>+</sup> resting T cells or actively-proliferating encephalitogenic T cells were analyzed in outsourcing for metabolic profile by Metabolon. Bioinformatics analysis was performed as described in

“Materials and methods”. (A) Volcano plot was obtained by plotting the log<sub>2</sub> ratio of mean values for the 158 metabolites profiled in the metabolomics analysis (fold change of metabolite concentration in encephalitogenic T cells over resting T cells; see **Table I**), against the negative log<sub>10</sub> of the *P*-value from the Student’s *t*-test. Metabolite concentrations that changed significantly (*P*<0.05) are indicated in red if upregulated and green if downregulated. (B) Heatmap of 89 metabolites significantly differing between resting and encephalitogenic T cells as revealed by statistical analysis. (C) Results of the bioinformatics analysis performed with Metscape as described in “Materials and methods” section. A representative subnetwork of potentially important metabolites associated with metabolic reprogramming of actively-proliferating encephalitogenic T cells is shown. Red and green nodes represent higher and lower metabolite intracellular levels in actively-proliferating encephalitogenic T cells compared to resting T cells, respectively. Clusters of metabolites associated with specific metabolic pathways are depicted.



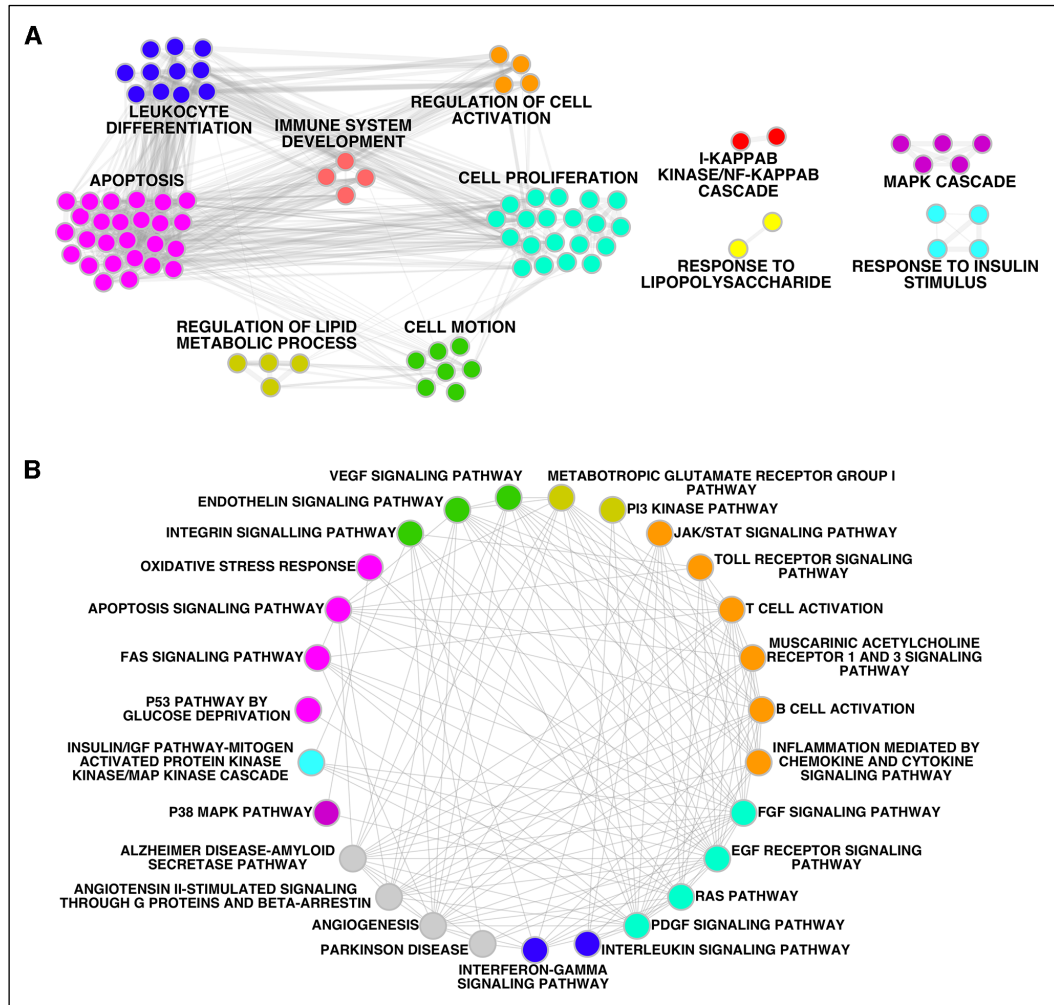
**Figure 8. Chemical structure of the low-molecular weight thiol pantethine.** Pantethine is the metabolically active form of pantothenic acid (commonly known as vitamin B5), and is made of two pantothenic acid molecules linked together by disulfide cysteamine. Pantethine also represents the stable disulfate form of pantetheine, and is formed by two pantetheine molecules linked by a disulfide bridge.



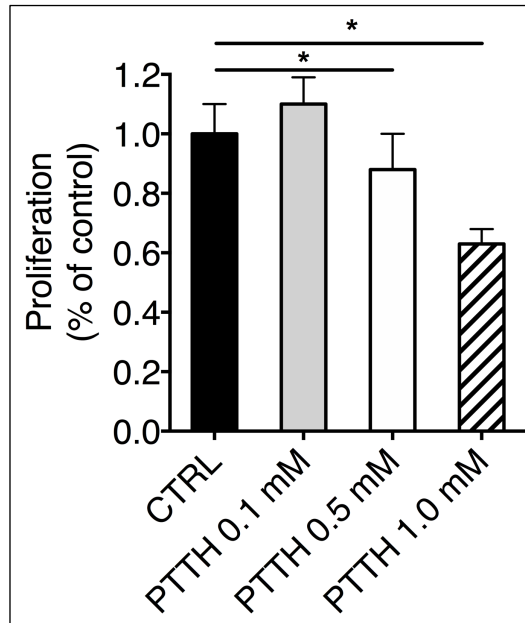


**Figure 9. Metabolomics analysis showed drastic metabolic reprogramming in actively-proliferating encephalitogenic T cells as a consequence of CoA fueling induced by pantothenine.** Actively-proliferating encephalitogenic T cells were treated with pantothenine 1.0 mM for 6 hours and analyzed in outsourcing for metabolic profile by Metabolon. Bioinformatics analysis was performed on raw data from Metabolon, as described in the “Materials and methods” section. (A) Volcano plot was obtained by plotting the  $\log_2$  ratio of mean values for the 158 biochemicals profiled in the metabolomics analysis (fold change of metabolite concentration in encephalitogenic T cells treated with pantothenine over

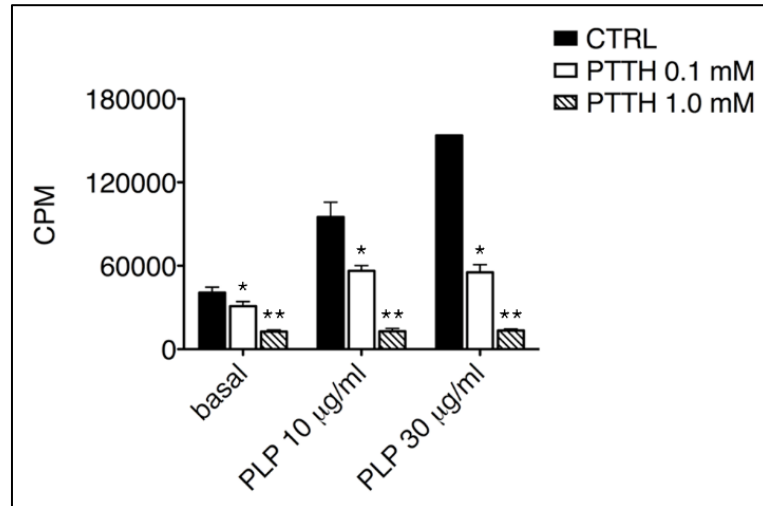
encephalitogenic control T cells; see **Table I**), against the negative  $\log_{10}$  of the  $P$ -value from the Student's t-test. Proteins that changed significantly ( $P < 0.05$ ) are indicated in red if upregulated and green if downregulated. (B) Heatmap of 48 metabolites ( $P < 0.05$ ) significantly modified following CoA fueling with pantethine. (C) Results of the bioinformatics analysis performed with Metscape as described in "Materials and methods" section. A representative subnetwork of potentially important metabolites associated with the metabolic reprogramming of actively-proliferating encephalitogenic T cell induced by CoA fueling with pantethine. Red and green nodes represent higher and lower metabolites' intracellular levels in actively-proliferating encephalitogenic T cells treated with pantethine compared to untreated cells, respectively. [PTTH: pantethine]



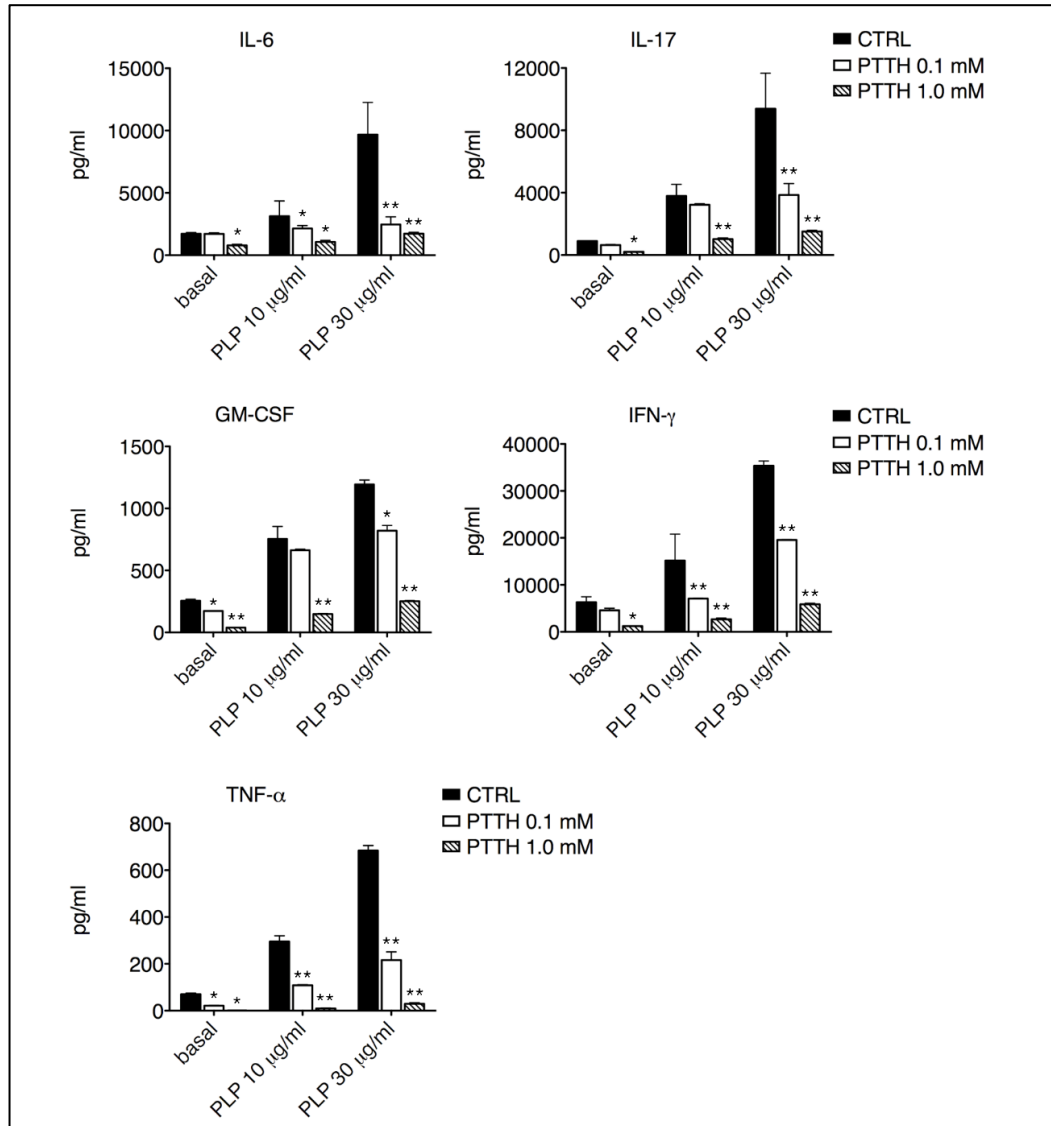
**Figure 10. Phosphoproteomics study suggested an immuno-modulatory effect of pantethine on encephalitogenic T cells.** Actively-proliferating encephalitogenic T cells were treated with pantethine 1.0 mM for 6 hours and analyzed in outsourcing for total protein expression and phosphorylation by Kinexus (see **Table II** for protein dataset). On raw data from Kinexus, a bioinformatics analysis was then performed as described in “Materials and methods” section. Network representation of Gene Ontology (GO) analysis (A) and PANTHER pathways analysis (B) on proteins modified by pantethine treatment are shown. Nodes represent terms and edges connect two terms that share at least a protein. Nodes with a specific color in the PANTHER pathways network are associated with terms of the GO network bearing the same color.



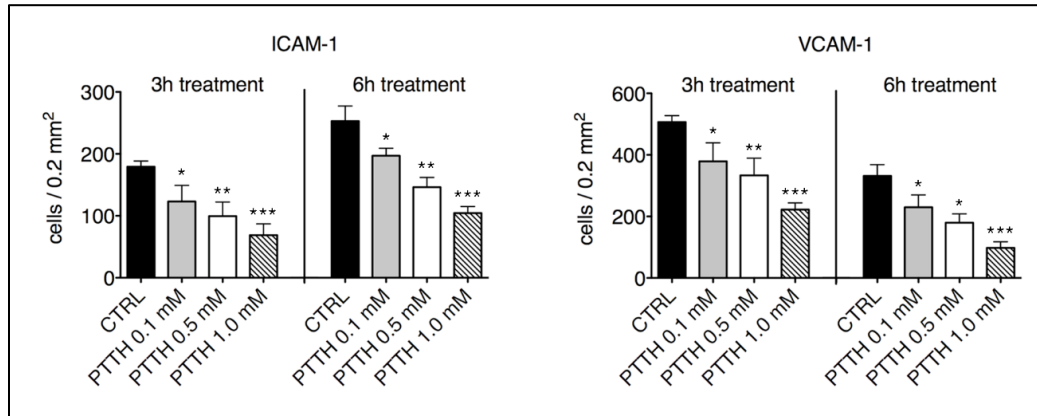
**Figure 11. Pantethine inhibited actively-proliferating encephalitogenic T cell proliferation rate *in vitro*.** Actively-proliferating encephalitogenic T cells were treated with pantethine 1.0 mM for 6 hours, washed, re-seeded and left to proliferate for further 18 hours. Pantethine treatment inhibits encephalitogenic T cell proliferative response in a dose-dependent manner, compared to control cells ( $*P<0.05$ ). Data are the mean  $\pm$  standard error of the mean (SEM) of three independent experiments performed in triplicate. [CTRL: control; PTTH: pantethine]



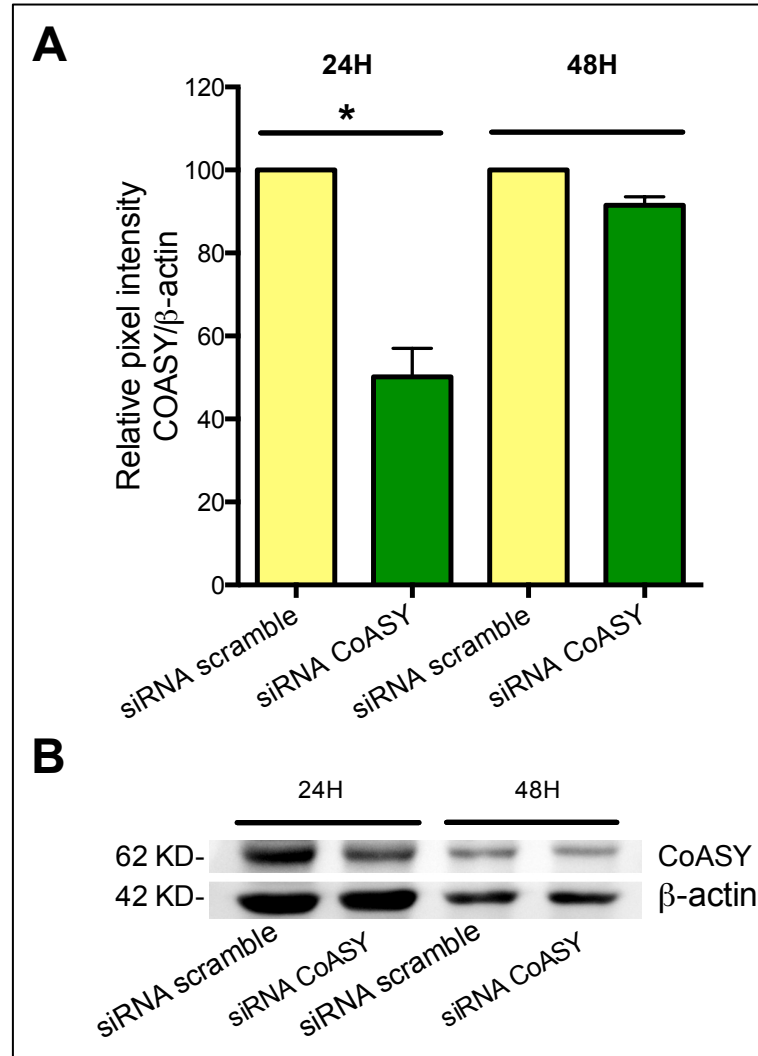
**Figure 12. Pantethine inhibited encephalitogenic T cell proliferation after antigen-stimulation *in vitro*.** PLP<sub>139-151</sub>-specific T cells were treated with PBS (control cells) or pantethine 0.1 or 1.0 mM for 16 hours before re-stimulation with different antigen (PLP<sub>139-151</sub>) concentrations, in the presence of irradiated splenocytes as APCs. Pantethine pre-treatment strongly inhibited encephalitogenic T cell proliferative response in a dose-dependent manner, when compared to control cells (\* $P < 0.05$  and \*\* $P < 0.01$  compared to the corresponding control condition). Data are the mean  $\pm$  SEM of three independent experiments. [CTRL: control; PTTH: pantethine]



**Figure 13. Pantethine inhibited pro-inflammatory cytokine production by encephalitogenic T cell proliferation.** Supernatants from proliferation assays depicted in Figure 12 were collected, and cytokine content was evaluated with the Bio-plex system. Pantethine pre-treatment inhibited the production of IL-6, IL-17, GM-CSF, IFN- $\gamma$  and TNF- $\alpha$  by PLP<sub>139-151</sub>-specific T cell lines following *in vitro* re-stimulation (\* $P$ <0.05 and \*\* $P$ <0.01 compared to the corresponding control condition). Data are the mean  $\pm$  standard deviation (SD) of one representative experiment performed in triplicate. [CTRL: control; PTTH: pantethine]

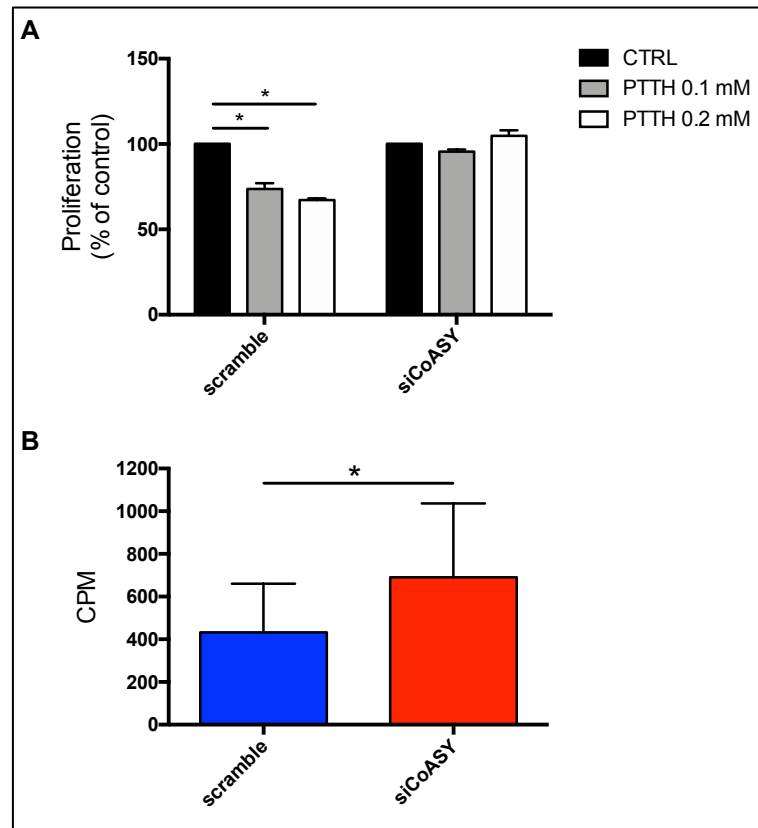


**Figure 14. Pantethine reduced integrin-dependent encephalitogenic T cell adhesion *in vitro*.** Activated PLP<sub>139-151</sub>-specific T cells were treated with PBS (control cells) or pantethine 0.1, 0.5 or 1.0 mM for 3 or 6 hours. Cells were then left spontaneously adhere on glass slides pre-coated with ICAM-1 or VCAM-1 1 µg/ml. Pantethine inhibited integrin-mediated adhesion of encephalitogenic T cells in a dose-dependent manner (\* $P < 0.05$ , \*\* $P < 0.01$  and \*\*\* $P < 0.001$  compared to the corresponding control condition). Data are the mean  $\pm$  SEM of three independent experiments. [CTRL: control; PTTH: pantethine]



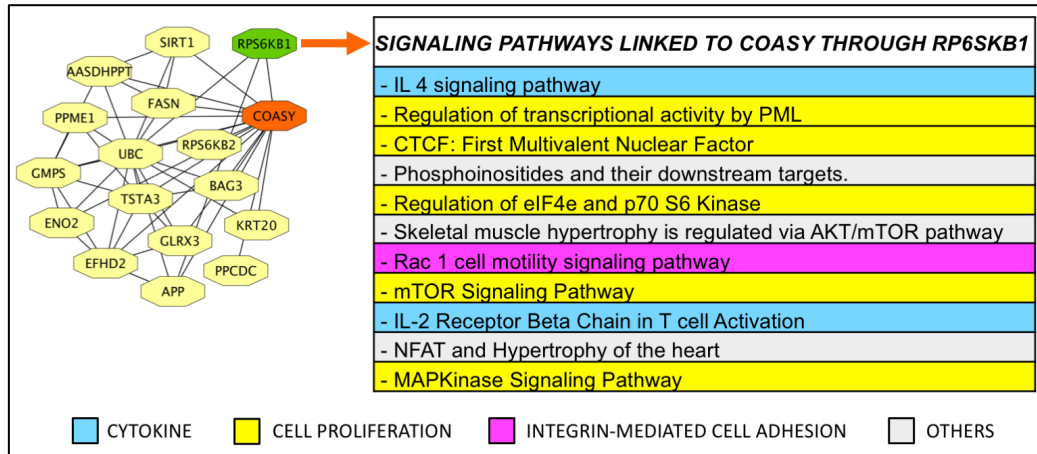
**Figure 15. Western blot demonstrating silencing of CoASY in our experimental setting.** Low-proliferating PLP<sub>139-151</sub>-specific T cells were transfected with either siRNA against CoASY or siRNA-scramble as control, and the silencing was evaluated after 24 hours (24H) or 48 hours (48H) post transfection by western blot analysis. A) Relative quantification of the western blots band intensities. Values represent the mean  $\pm$  SEM of three independent experiments ( $*P < 0.05$  versus control). We observed that the knockdown efficiency of CoASY was around 50% after 24 hours, whereas it was not effective at 48 hours. B) Representative western-blot showing the reduction in CoASY expression 24H but not 48H post-transfection, compared to siRNA-scramble.  $\beta$ -actin was used as control housekeeping gene.



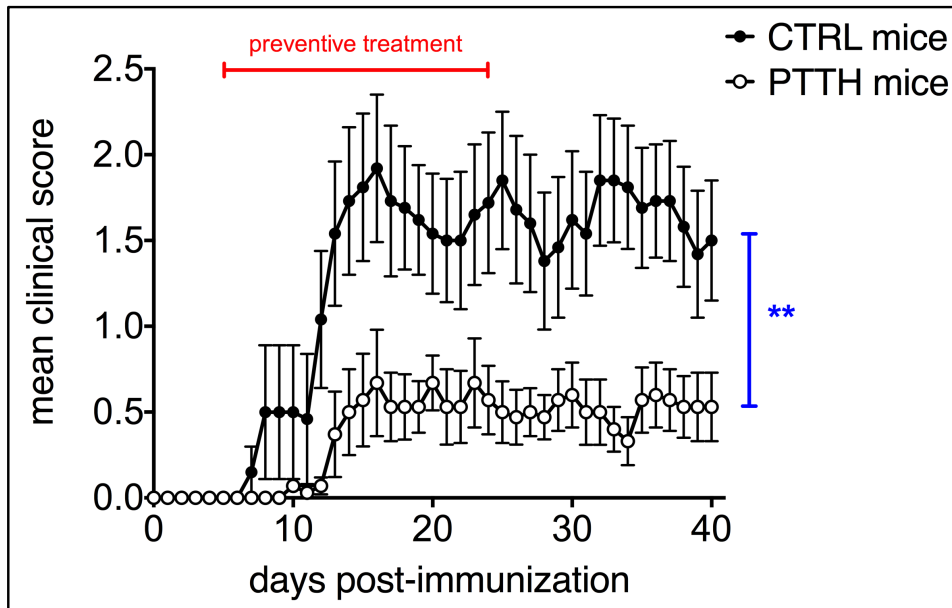


**Figure 16. CoASY silencing reduced the inhibitory effect of pantethine on the proliferation of encephalitogenic T cells and increases basal proliferative capacity.** Low-proliferating PLP<sub>139-151</sub>-specific T cells were transiently transfected with siRNA-CoASY or control scramble siRNA. A) Within 24 hours post transfection cells were treated with PBS (control cells) or pantethine 0.1 or 0.2 mM for 16 hours before re-stimulation with PLP<sub>139-151</sub> peptide, in the presence of irradiated splenocytes as APCs. Proliferation assay showed that siRNA-CoASY-transfected cells were no more sensitive to pantethine treatment following antigen restimulation, compared to siRNA scramble-transfected cells (\* $P < 0.05$  compared to the corresponding control condition). B) The proliferation assays showed that transfection with a siRNA-CoASY increased the basal proliferation of unstimulated PLP<sub>139-151</sub>-specific T cells, compared to control siRNA-transfected cells (\* $P < 0.05$ ).

Data are the mean  $\pm$  SEM of three independent experiments. [CTRL: control; PTTH: pantethine]



**Figure 17. CoASY – RPS6KB1 complex links metabolism to immune related signaling pathways.** We analyzed a PPI network centered on CoASY (left). The PPI network of CoASY was built using Cytoscape software and a network database of known and predicted PPI (see “Materials and methods” section). Then, with the Cytoscape plug-in JEPETTO we performed an enrichment analysis of the signaling pathways in which CoASY and its first interacting proteins were involved. From the bioinformatics analysis, RPS6KB1 (green node of the network) resulted as the most important linker protein of CoASY (orange node) with immune related signaling pathways (table on the right). Data obtained suggested that direct interaction between CoASY and RPS6KB1 may have a role in the regulation of signaling pathways related to cell proliferation (yellow), cytokine production (cyan), cell motility (magenta) mainly through effects on Mapk, Rac1 and MTOR pathways.





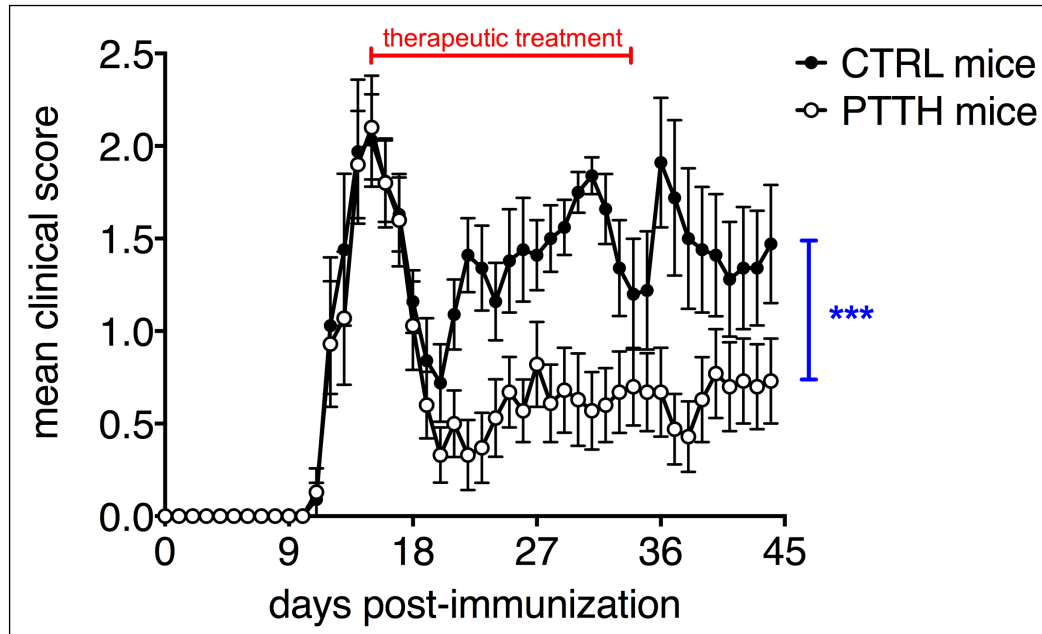


**Figure 18. Preventive treatment with pantethine inhibited RR-EAE development in SJL mice.** PLP<sub>139-151</sub> EAE-immunized mice were treated *per os* with 30 mg/day of pantethine from day +5 post-immunization for 20 consecutive days (red line). PTTH treatment reduced incidence, maximal clinical score and cumulative score, compared to untreated animals (CTRL mice) (see also **Table III** for quantification; \*\* $P < 0.01$  compared to the CTRL animals). Data are the mean  $\pm$  SEM of three independent experiments. [CTRL: control; PTTH: pantethine]



**Figure 19. Therapeutic treatment with pantethine ameliorated established RR-EAE clinical course in SJL mice.** PLP<sub>139-151</sub> EAE-immunized mice were treated *per os* with 30 mg/day of pantethine from day +18 post-immunization (after the first disease relapse) for 20 consecutive days (red line). PTTH treatment reduced the number of relapses and the post-treatment cumulative score and mean maximum score, compared to untreated animals (control mice) (see also **Table IV** for quantification; \*\*\* $P < 0.001$  compared to the control animals). Data are the mean  $\pm$  SEM of two independent experiments.

[CTRL: control; PTTH: pantethine]

**Table I. Summary of metabolites affected by pantethine treatment in PLP139-151-specific encephalitogenic T cells.** The table includes results of statistical tests with associated heat maps, *P*-values, and mean values from metabolomics analysis. The dataset below includes a total of 158 compounds of known identity (named biochemicals). Following normalization to protein concentration, log transformation and imputation with minimum observed values for each compound (analysis provided by Metabolon), Welch's two-sample *t*-test was used to identify biochemicals that differed significantly between experimental groups. A summary of the numbers of biochemicals that achieved statistical significance ( $p \leq 0.05$ ), as well as those approaching significance ( $0.05 < P < 0.10$ ), is shown.

Comparison mean values significantly different:		Comparison mean values approaching significance:	
	$p \leq 0.05$ , fold of change $\geq 1.00$		$0.05 < p < 0.10$ , fold of change $\geq 1.00$
	$p \leq 0.05$ , fold of change $< 1.00$		$0.05 < p < 0.10$ , fold of change $< 1.00$

<i>Heat map of statistically significant biochemicals profiled in this study.</i>			Welch's Two-Sample t-Test						
			Fold of Change		P-values		Mean Values		
Super Pathway	Sub Pathway	Biochemical Name	PLP Ctrl vs Resting Ctrl	PLP PTTH 6h vs PLP Ctrl	PLP Ctrl 6h / Resting Ctrl 6h	PLP PTTH 6h / PLP Ctrl 6h	Resting Ctrl 6h	PLP Ctrl 6h	PLP PTTH 6h
Amino acid	Glycine, serine and threonine metabolism	glycine	0.13	0.71	0.025	0.011	9.033	1.166	0.828
		serine	0.70	0.76	0.961	0.040	1.756	1.234	0.934
		threonine	0.49	0.80	0.459	0.087	2.430	1.187	0.952
		Isobar: betaine aldehyde, N-methyldiethanolamine	0.01	1.02	0.001	0.857	69.053	0.652	0.662
	Alanine and aspartate metabolism	aspartate	0.04	0.89	0.005	0.162	26.901	1.180	1.055
		asparagine	0.29	1.03	0.047	0.776	3.529	1.029	1.062
		alanine	0.53	0.85	0.474	0.057	2.155	1.137	0.969
		N-carbamoylaspartate	4.35	0.43	0.000	0.002	0.157	0.683	0.296
		N-acetylaspartate (NAA)	1.81	0.73	0.112	0.165	0.692	1.251	0.916
	Glutamate metabolism	glutamate	0.23	0.87	0.072	0.004	4.357	0.982	0.859
		glutamine	0.24	0.63	0.048	0.000	4.459	1.089	0.689

Histidine metabolism	histidine	0.44	<b>0.72</b>	0.433	0.005	2.591	1.139	0.819
	histamine	<b>1.45</b>	1.01	0.002	0.884	0.670	0.970	0.976
Lysine metabolism	lysine	1.12	<b>0.75</b>	0.434	0.017	1.019	1.144	0.863
Phenylalanine & tyrosine metabolism	phenylalanine	1.34	0.90	0.257	0.128	0.782	1.047	0.939
	tyrosine	1.21	<b>0.84</b>	0.338	0.002	0.938	1.136	0.957
Tryptophan metabolism	kynurenine	<b>2.51</b>	0.76	0.006	0.165	0.523	1.312	1.001
	tryptophan	0.80	<b>0.82</b>	0.925	0.078	1.363	1.090	0.896
	serotonin (5HT)	<b>32.88</b>	1.08	0.004	0.134	0.030	0.996	1.078
Valine, leucine and isoleucine metabolism	isoleucine	0.52	<b>0.87</b>	0.463	0.095	2.047	1.057	0.922
	leucine	0.75	<b>0.80</b>	0.867	0.006	1.517	1.142	0.911
	valine	0.95	<b>0.80</b>	0.622	0.001	1.230	1.165	0.933
	hypotaurine	0.39	<b>1.42</b>	0.262	0.000	1.888	0.728	1.036
	taurine	<b>0.21</b>	1.02	0.099	0.640	3.731	0.772	0.789
	S-adenosylmethionine (SAM)	0.89	<b>0.85</b>	0.856	0.059	1.497	1.331	1.131
	S-adenosylhomocysteine (SAH)	0.83	<b>1.70</b>	0.688	0.002	0.910	0.753	1.279
	methionine	0.36	<b>0.89</b>	0.330	0.070	2.675	0.962	0.860
Urea cycle; arginine-, proline-, metabolism	asymmetric dimethylarginine (ADMA)	0.87	<b>0.59</b>	0.857	0.007	1.693	1.475	0.876
	arginine	0.46	<b>0.89</b>	0.412	0.024	2.176	1.007	0.895
	urea	<b>0.28</b>	1.00	0.003	0.995	3.457	0.953	0.951
	proline	0.36	<b>0.78</b>	0.287	0.005	3.356	1.199	0.934
	citrulline	<b>2.63</b>	1.01	0.071	0.871	0.686	1.803	1.813

	trans-4-hydroxyproline	0.41	<b>1.09</b>	0.228	0.057	2.494	1.013	1.101
Creatine metabolism	creatine	0.51	<b>0.85</b>	0.534	0.071	2.237	1.134	0.965
	spermine	<b>0.29</b>	1.11	0.056	0.227	3.173	0.925	1.023
Guanidino and acetamido metabolism	4-guanidinobutanoate	0.23	<b>0.56</b>	0.124	0.003	5.800	1.347	0.751
Glutathione metabolism	glutathione, reduced (GSH)	0.39	<b>1.11</b>	0.172	0.092	2.400	0.932	1.037
	5-oxoproline	<b>0.04</b>	<b>1.54</b>	0.012	0.019	14.484	0.596	0.918
	glutathione, oxidized (GSSG)	0.89	<b>1.65</b>	0.952	0.003	1.057	0.946	1.557
	glycylleucine	<b>7.85</b>	1.23	0.000	0.145	0.126	0.989	1.219
	glycylphenylalanine	<b>1.69</b>	<b>1.46</b>	0.007	0.015	0.513	0.865	1.262
	alanylleucine	<b>2.06</b>	0.93	0.001	0.378	0.533	1.099	1.026
	alanylphenylalanine	<b>1.96</b>	0.92	0.003	0.384	0.516	1.009	0.924
	asparagylleucine	<b>5.36</b>	1.08	0.000	0.463	0.211	1.132	1.227
	alanyltyrosine	<b>4.41</b>	0.94	0.000	0.477	0.266	1.176	1.100
	aspartylphenylalanine	<b>3.32</b>	1.01	0.000	0.963	0.325	1.079	1.085
	alpha-glutamylglutamate	<b>2.91</b>	0.79	0.062	0.102	0.441	1.283	1.012
	glutamine-leucine	<b>2.80</b>	1.10	0.000	0.323	0.379	1.060	1.166
	leucylleucine	<b>3.30</b>	1.02	0.000	0.880	0.329	1.087	1.110
	threonylisoleucine	1.12	<b>1.80</b>	0.195	0.001	0.485	0.542	0.975
	threonylphenylalanine	<b>3.99</b>	0.88	0.000	0.148	0.277	1.107	0.970
	valylphenylalanine	<b>2.96</b>	0.94	0.000	0.546	0.394	1.168	1.097
	cysteinylglycine	<b>0.39</b>	0.96	0.080	0.806	2.545	1.002	0.966
	tyrosylvaline	<b>1.52</b>	<b>1.44</b>	0.056	0.053	0.568	0.863	1.242



	arginylisoleucine	1.38	1.84	0.014	0.001	0.625	0.864	1.588
	arginylleucine	1.60	1.17	0.002	0.040	0.598	0.955	1.114
	arginylglutamate	1.75	1.45	0.005	0.014	0.506	0.886	1.283
	aspartylleucine	2.99	1.02	0.000	0.908	0.338	1.009	1.026
	histidylleucine	12.92	1.09	0.000	0.040	0.083	1.070	1.170
	isoleucylalanine	3.11	0.98	0.000	0.820	0.342	1.063	1.043
	isoleucylglutamine	2.81	1.02	0.001	0.890	0.383	1.074	1.090
	isoleucylphenylalanine	4.30	1.04	0.001	0.697	0.254	1.093	1.136
	isoleucylvaline	1.63	0.99	0.002	0.927	0.602	0.984	0.978
	leucylalanine	2.95	1.25	0.001	0.099	0.304	0.898	1.121
	leucylglycine	2.77	1.14	0.001	0.323	0.341	0.945	1.077
	lysylisoleucine	2.42	0.82	0.001	0.054	0.482	1.168	0.957
	lysylleucine	1.54	0.95	0.001	0.561	0.674	1.037	0.980
	phenylalanylleucine	2.47	0.97	0.003	0.854	0.439	1.087	1.057
	phenylalanylserine	1.50	1.92	0.067	0.011	0.427	0.641	1.231
	serylleucine	2.99	1.26	0.001	0.074	0.307	0.919	1.157
	serylphenylalanine	2.41	1.12	0.005	0.447	0.432	1.039	1.168
	threonylleucine	3.42	0.97	0.000	0.698	0.318	1.087	1.049
	tyrosylleucine	4.33	0.91	0.001	0.471	0.305	1.322	1.202
	tyrosylglycine	1.56	1.30	0.003	0.041	0.607	0.945	1.231
	alpha-glutamyltyrosine	2.45	1.02	0.052	0.871	0.451	1.104	1.125
	phenylalanylaspargate	1.81	1.24	0.009	0.162	0.512	0.925	1.149
gamma-glutamyl	gamma-glutamylglutamate	0.10	0.97	0.008	0.777	9.009	0.900	0.876

	N-acetylneuraminate	1.50	1.01	0.002	0.824	0.688	1.032	1.046
	Isobar: UDP-acetylglucosamine, UDP-acetylgalactosamine	0.22	0.98	0.040	0.871	3.943	0.886	0.871
Fructose, mannose, galactose, starch, and sucrose metabolism	6'-sialyllactose	2.31	1.27	0.082	0.340	0.418	0.964	1.226
	mannose-6-phosphate	3.56	0.66	0.047	0.034	0.408	1.451	0.955
	maltopentaose	2.67	1.06	0.001	0.539	0.394	1.052	1.112
	maltohexaose	2.45	1.14	0.000	0.125	0.405	0.992	1.129
Oligosaccharide	maltotetraose	2.92	1.08	0.001	0.440	0.361	1.055	1.138
Glycolysis, gluconeogenesis, pyruvate metabolism	glucose-6-phosphate (G6P)	3.48	0.75	0.030	0.137	0.411	1.432	1.071
	glucose	2.50	0.70	0.006	0.141	0.612	1.530	1.068
	fructose-6-phosphate	2.76	0.88	0.061	0.390	0.543	1.501	1.319
	Isobar: fructose 1,6-diphosphate, glucose 1,6-diphosphate, myo-inositol 1,4 or 1,3-diphosphate	0.23	0.67	0.009	0.294	5.145	1.166	0.778
	lactate	0.68	0.87	0.920	0.089	1.704	1.156	1.006
Nucleotide sugars, pentose metabolism	6-phosphogluconate	0.13	1.89	0.008	0.000	6.768	0.868	1.641
	sedoheptulose-7-phosphate	5.45	0.48	0.067	0.253	0.193	1.052	0.510
	ribose 5-phosphate	0.95	0.95	0.689	0.722	1.221	1.162	1.103
	Isobar: ribulose 5-phosphate, xylulose 5-phosphate	2.50	0.77	0.013	0.151	0.527	1.316	1.011

	Nucleotide sugars	UDP-glucose (isobar with UDP-galactose)	0.18	1.38	0.044	0.013	4.053	0.715	0.990
Energy	Krebs cycle	citrate	0.69	0.86	0.953	0.203	1.436	0.998	0.854
		fumarate	0.25	0.78	0.059	0.146	2.957	0.740	0.579
		malate	0.21	0.86	0.030	0.214	4.678	0.985	0.842
	Oxidative phosphorylation	phosphate	0.25	0.92	0.056	0.311	3.732	0.926	0.849
		linolenate [alpha or gamma; (18:3n3 or 6)]	1.62	0.95	0.006	0.602	0.578	0.937	0.891
	Long chain fatty acid	palmitoleate (16:1n7)	1.61	0.88	0.138	0.036	0.621	1.003	0.885
		eicosenoate (20:1n9 or 11)	0.24	0.93	0.084	0.336	3.250	0.777	0.719
		dihomo-linoleate (20:2n6)	0.28	0.86	0.052	0.434	3.444	0.974	0.839
		mead acid (20:3n9)	9.97	1.09	0.001	0.576	0.111	1.107	1.206
		arachidonate (20:4n6)	0.38	1.24	0.199	0.309	2.013	0.773	0.957
		docosadienoate (22:2n6)	0.26	1.11	0.075	0.009	2.921	0.766	0.854
	Fatty acid, amide	stearamide	0.54	0.89	0.052	0.594	1.564	0.845	0.750
	Carnitine metabolism	deoxycarnitine	0.08	1.13	0.012	0.157	9.738	0.818	0.921
		carnitine	0.03	0.74	0.004	0.002	45.822	1.209	0.900
		acetylcarnitine	0.08	0.99	0.011	0.948	11.002	0.855	0.848
	Glycerolipid metabolism	choline phosphate	0.08	0.94	0.013	0.245	8.830	0.732	0.690
		phosphoethanolamine	0.13	0.87	0.013	0.051	8.056	1.037	0.906
		glycerophosphorylcholine (GPC)	0.39	1.32	0.174	0.002	1.999	0.775	1.023

		cytidine 5'-diphosphocholine	0.14	1.28	0.016	0.034	5.592	0.801	1.026
	Inositol metabolism	myo-inositol	0.09	0.80	0.001	0.443	9.997	0.881	0.703
	Lysolipid	1-palmitoylglycerophosphoethanolamine	0.15	0.73	0.055	0.039	6.398	0.965	0.703
		1-stearoylglycerophosphoethanolamine	0.22	0.91	0.071	0.112	4.214	0.911	0.825
		2'-arachidonoylglycerophosphoethanolamine	0.19	1.26	0.068	0.554	3.554	0.673	0.846
		lanosterol	2.29	1.15	0.053	0.435	0.338	0.776	0.891
Nucleotide	Purine metabolism, (hypo)xanthine/inosine containing	xanthine	2.03	0.74	0.111	0.025	0.620	1.258	0.929
		hypoxanthine	0.20	0.85	0.109	0.056	4.722	0.967	0.822
		inosine	0.17	0.96	0.011	0.622	6.209	1.050	1.004
		2'-deoxyinosine	7.06	0.62	0.001	0.038	0.232	1.638	1.010
		inosine 5'-monophosphate (IMP)	0.04	0.81	0.000	0.441	21.126	0.799	0.647
	Purine metabolism, adenine containing	adenine	0.72	1.01	0.552	0.995	1.630	1.172	1.182
		adenosine	0.13	1.00	0.027	0.980	7.011	0.912	0.916
		2'-deoxyadenosine 3'-monophosphate	4.89	0.86	0.001	0.350	0.268	1.311	1.124
		adenosine 3'-monophosphate (3'-AMP)	1.51	0.76	0.002	0.001	0.720	1.087	0.824
		adenosine 5'-monophosphate (AMP)	0.07	1.20	0.002	0.391	11.039	0.817	0.982

		adenylosuccinate	0.15	0.72	0.071	0.130	6.951	1.069	0.768
Purine metabolism, guanine containing		guanine	0.04	0.67	0.012	0.260	27.046	1.065	0.714
		7-methylguanine	1.56	1.40	0.179	0.013	0.693	1.083	1.515
		guanosine	0.14	1.08	0.005	0.565	6.385	0.924	0.994
		2'-deoxyguanosine	2.96	0.60	0.007	0.047	0.534	1.583	0.942
		guanosine 5'- monophosphate (5'-GMP)	0.08	1.02	0.001	0.795	11.590	0.898	0.912
Purine metabolism, urate metabolism		urate	2.20	1.13	0.038	0.602	0.519	1.142	1.290
Pyrimidine metabolism, cytidine containing		cytidine	0.12	0.97	0.030	0.891	7.256	0.850	0.828
		cytidine 5'-monophosphate (5'-CMP)	0.21	1.28	0.027	0.091	3.829	0.801	1.028
Pyrimidine metabolism, orotate containing		orotate	6.36	0.45	0.000	0.020	0.155	0.984	0.445
Pyrimidine metabolism, thymine containing		thymidine	0.45	0.60	0.660	0.008	2.634	1.185	0.711
Pyrimidine metabolism, uracil containing		uracil	0.62	0.91	0.722	0.096	1.896	1.180	1.077
		uridine	0.03	0.77	0.026	0.109	27.247	0.945	0.729
		uridine monophosphate (5' or 3')	0.28	1.21	0.024	0.136	3.849	1.082	1.305
Cofactors and vitamins	Ascorbate and aldarate metabolism	ascorbate (Vitamin C)	0.30	1.00	0.069		2.100	0.633	0.633
	Nicotinate and	nicotinamide	0.24	0.80	0.139	0.074	4.476	1.078	0.858

	nicotinamide metabolism	adenosine 5'diphosphoribose	<b>2.04</b>	<b>0.63</b>	0.008	0.019	0.434	0.887	0.560
	Pantothenate and CoA metabolism	pantothenate	<b>0.14</b>	<b>32.88</b>	0.030	0.000	0.358	0.051	1.674
		CoA	<b>0.23</b>	<b>0.60</b>	0.022	0.001	4.577	1.071	0.640
		3'-dephospho-CoA	<b>3.40</b>	<b>0.75</b>	0.012	0.001	0.445	1.511	1.127
	Riboflavin metabolism	flavin adenine dinucleotide (FAD)	<b>0.34</b>	0.94	0.063	0.233	2.553	0.881	0.826
	Thiamine metabolism	thiamin (Vitamin B1)	<b>2.38</b>	<b>1.34</b>	0.000	0.000	0.400	0.954	1.274
	Tocopherol metabolism	alpha-tocopherol	0.96	<b>2.16</b>	0.784	0.026	0.474	0.456	0.984
Xenobiotics	Chemical	glycerol 2-phosphate	<b>2.07</b>	0.91	0.066	0.257	0.495	1.026	0.933
		2-ethylhexanoate (isobar with 2-propylpentanoate)	<b>0.13</b>	1.20	0.014	0.358	5.018	0.652	0.785
		phenol red	0.62	1.18	0.257	0.147	1.177	0.730	0.858
	Drug	penicillin G	0.44	<b>0.90</b>	0.189	0.075	1.826	0.798	0.719
		streptomycin	<b>2.02</b>	0.94	0.100	0.460	0.540	1.093	1.031
		Gentamycin	<b>6.40</b>	1.05	0.000	0.609	0.165	1.053	1.101
	Sugar, sugar substitute, starch	erythritol	0.28	<b>0.66</b>	0.146	0.082	3.486	0.990	0.655

**Table II. Analysis of phosphoproteomics data.** “Pan-Specific” antibodies determine expression value, whereas the others account for specific phosphorylation site (e.g. Y1034, T183, S780; Y: tyrosine, T: threonine, S: serine). Z-score refers to the ratios of actively-proliferating PLP<sub>139-151</sub>-specific T cells treated with 1.0mM of pantethine versus control actively-proliferating PLP<sub>139-151</sub>-specific T cells treated with PBS. Green: downregulation; red: upregulation.

NAME	Z-Score	TYPE	NAME	Z-Score	TYPE
AXL	-7,53	Pan-specific	CRYAB	8,40	Pan-specific
CSNK2A1	-6,74	Pan-specific	RB1	6,42	S780
ATF2	-5,72	Pan-specific	PAK1	6,06	Pan-specific
CAMK4	-5,31	Pan-specific	GRIN2B	5,44	Y1474
MAPK10	-5,08	Pan-specific	NFKBIB	4,53	Pan-specific
CDK6	-5,03	Pan-specific	TLK1	4,22	Pan-specific
CASP4	-4,98	Pan-specific	DNAJB1	4,12	Pan-specific
BRCA1	-4,59	S1497	PPP6C	4,02	Pan-specific
CAMKK1	-4,54	Pan-specific	NLK	3,90	Pan-specific
EEF2K	-4,23	Pan-specific	MAPK14	3,79	T180+Y182
HMOX1	-4,15	Pan-specific	MAP2K3	3,73	S218/S207
BUB1	-4,12	Pan-specific	DDR2	3,67	Pan-specific
PLK2	-4,08	Pan-specific	ZAP70	3,47	Y319/Y352
CALR	-3,89	Pan-specific	AKT2	3,43	Pan-specific
HIST1H1A	-3,81	phospho CDK1 sites	PRKCH	3,40	Pan-specific
YWHAZ	-3,64	Pan-specific	DUSP1	3,29	Pan-specific
STK17B	-3,62	Pan-specific	GRIN1	3,20	S896
AURKC	-3,61	Pan-specific	NTRK1	3,18	Pan-specific
MAP3K5	-3,60	Pan-specific	PTEN	3,17	Pan-specific
PRKAA1	-3,34	T183	CCNA1	2,98	Pan-specific
PRKDC	-3,26	Pan-specific	MAPK12	2,96	Pan-specific
DAPK2	-3,18	Pan-specific	PKN2	2,94	Pan-specific
RIPK4	-3,14	Pan-specific	RPS6KA1	2,91	S363/S369
CANX	-3,03	Pan-specific	ARAF	2,89	Pan-specific
ACACA	-2,99	S80	SOD1	2,85	Pan-specific
TNK2	-2,93	Pan-specific	PPP2R2C	2,84	Pan-specific
CAV2	-2,82	Pan-specific	RAF1	2,84	S259
CSNK1E	-2,82	Pan-specific	PRK CZ	2,83	T410/T412
MAP2K4	-2,75	S257+T261	CDK8	2,75	Pan-specific

PTPN6	-2,74	Pan-specific	PTK2B	2,73	Pan-specific
MAPK7	-2,68	Pan-specific	VRK1	2,72	Pan-specific
PDIA4	-2,45	Pan-specific	TBK1	2,70	Pan-specific
GNB2L1	-2,44	Pan-specific	CDK5	2,62	Pan-specific
PRKG1	-2,37	Pan-specific	PPP1CB	2,57	Pan-specific
MAP3K8	-2,36	Pan-specific	MAP2K6	2,57	S207
ST13	-2,32	Pan-specific	TEK	2,48	Pan-specific
CAMK2B	-2,30	Pan-specific	DAPK3	2,45	Pan-specific
CDC25B	-2,30	Pan-specific	MAP3K7	2,45	Pan-specific
H3F3B	-2,23	T4	PDPK1	2,43	Pan-specific
PRKACA	-2,20	T198	AKT3	2,43	Pan-specific
MAPK9	-2,19	Pan-specific	STK33	2,39	Pan-specific
Rac1	-2,13	Pan-specific	SRC	2,39	Pan-specific
RAD23B	-2,10	Pan-specific	STK4	2,37	Pan-specific
PRKD1	-2,03	S910	RPS6KA5	2,37	S376
TAOK3	-1,99	Pan-specific	SPHK1	2,37	Pan-specific
CASK	-1,98	Pan-specific	PRKAR2A	2,35	S99
CASP6	-1,98	Pan-specific	ROR2	2,32	Pan-specific
CDC42	-1,96	Pan-specific	PTPN11	2,28	S580
HMOX2	-1,93	Pan-specific	GSG2	2,16	Pan-specific
HSPA4	-1,91	Pan-specific	STRN3	2,15	Pan-specific
PPP4C	-1,89	Pan-specific	AKT1	2,12	S473
CAMK1D	-1,87	Pan-specific	PRKAB1	2,11	Pan-specific
MARCKS	-1,85	S159+S163	SPHK2	2,03	Pan-specific
ADD1	-1,85	S726	PDGFRB	1,99	Y716
HSPH1	-1,84	Pan-specific	HSP90AA1	1,99	Pan-specific
HSPA8	-1,75	Pan-specific	RPS6KB1	1,98	T412
GAP43	-1,72	S41	PRKCA	1,97	Pan-specific
ICK	-1,72	Pan-specific	TP53	1,97	Pan-specific
HSPA4L	-1,71	Pan-specific	STAT1	1,95	Pan-specific
MAPK3	-1,71	Pan-specific	SGK3	1,94	Pan-specific
HSPA1A	-1,69	Pan-specific	MAP2K2	1,92	Pan-specific
BMX	-1,67	Pan-specific	PIK3R4	1,91	Pan-specific
CAMK2G	-1,65	Pan-specific	MKNK2	1,88	Pan-specific
BAK1	-1,65	Pan-specific	MAP3K1	1,86	Pan-specific
CDC25C	-1,64	Pan-specific	MAP3K2	1,84	Pan-specific
CAMK2D	-1,63	Pan-specific	PKN1	1,83	Pan-specific
GSK3A	-1,63	Pan-specific	PDK2	1,81	Pan-specific
PTPN1	-1,62	Pan-specific	ROS1	1,78	Pan-specific
ILK	-1,60	Pan-specific	SOD2	1,77	Pan-specific
CAMK2A	-1,58	T286	STAT6	1,76	Pan-specific
CDKN3	-1,55	Pan-specific	CDKN1A	1,74	Pan-specific
CSE1L	-1,55	Pan-specific	MAP3K11	1,73	Pan-specific



JUN	-1,52	S73	PPM1D	1,73	Pan-specific
IGF1R	-1,46	Pan-specific	MYL12A	1,72	S19
CSNK1G2	-1,46	Pan-specific	PPP2R2A	1,71	Pan-specific
NFKBIA	-1,43	Pan-specific	HSPD1	1,69	Pan-specific
HSPB1	-1,43	S78	HSP90AB1	1,69	Pan-specific
MAP2K1	-1,42	Pan-specific	IRS1	1,69	Y1179
PPP2CA	-1,41	Pan-specific	PTPN21	1,68	Pan-specific
SYN1	-1,41	S9	EIF4E	1,66	S209
BAD	-1,40	S75	RAB5A	1,62	Pan-specific
HSP90B1	-1,38	Pan-specific	PACSIN1	1,62	Pan-specific
CDK4	-1,37	Pan-specific	P4HB	1,55	Pan-specific
ABL1	-1,36	Pan-specific	STAT3	1,53	Y705
AURKA	-1,34	Pan-specific	CDKN1B	1,52	Pan-specific
ANP32A	-1,33	Pan-specific	BCL2	1,52	Pan-specific
NPM1	-1,32	T199	TPTE2	1,50	Pan-specific
MAP2K5	-1,32	Pan-specific	DIABLO	1,49	Pan-specific
ARRB1	-1,31	Pan-specific	EGFR	1,48	Y1092
BCL2L1	-1,31	Pan-specific	NEK2	1,45	Pan-specific
IRAK2	-1,30	Pan-specific	STK25	1,44	Pan-specific
EIF4EBP1	-1,30	T45	FKBP4	1,43	Pan-specific
SET	-1,23	Pan-specific	MAP3K4	1,43	Pan-specific
AURKB	-1,23	Pan-specific	PRKCE	1,42	Pan-specific
CASP7	-1,23	Pan-specific	MYEF2	1,42	Pan-specific
CHUK	-1,23	Pan-specific	KSR1	1,41	Pan-specific
JAK1	-1,20	Pan-specific	BTK	1,38	Pan-specific
MAP4K5	-1,20	Pan-specific	SMAD2	1,38	Pan-specific
			MAPT	1,36	S739
			PPP5C	1,34	Pan-specific
			RPS6KA3	1,34	Pan-specific
			TYK2	1,32	Pan-specific
			CDKN2C	1,32	Pan-specific
			PRKCG	1,31	T655
			SOCS2	1,31	Pan-specific
			STAT5A	1,30	Pan-specific
			MYC	1,30	T58/S62
			PPP2R5A	1,25	Pan-specific
			CDK2	1,25	Pan-specific
			MET	1,24	Pan-specific
			PRKCD	1,24	Pan-specific
			DOK2	1,21	Y139
			PXN	1,20	Y118
			ERBB2	1,01	Pan-specific

**Table III. Clinical features of EAE mice treated with pantethine (preventive treatment).** [dpi: days post immunization]

	<b>% Incidence</b>	<b>Mean day of disease onset (dpi)</b>	<b>Mean maximum clinical score</b>	<b>Mean cumulative clinical score</b>
<b>CTRL mice</b>	100%	12.3 ± 3.1	2.7 ± 1.2	53.9 ± 44.4
<b>Pantethine-treated mice</b>	66,7%	14.7 ± 3.3	1.3 ± 1.2 <sup>a</sup>	16.5 ± 19.2 <sup>b</sup>
<sup>a</sup> <i>P</i> <0.005 compared to CTRL animals <sup>b</sup> <i>P</i> <0.007 compared to CTRL animals				

**Table IV. Clinical features of EAE mice treated with PTHH (therapeutic treatment).**

	<b>Mean maximum score pre-treatment</b>	<b>Mean cumulative score pre-treatment</b>	<b>Mean maximum score post-treatment</b>	<b>Mean cumulative score post-treatment</b>
<b>CTRL mice</b>	2.6 ± 1.1	12.0 ± 7.1	2.9 ± 1.3	35.2 ± 16.2
<b>Pantethine-treated mice</b>	2.4 ± 0.9	10.5 ± 6.2	1.3 ± 1.0 <sup>a</sup>	14.9 ± 16.2 <sup>b</sup>
<sup>a</sup> <i>P</i> <0.003 compared to CTRL animals <sup>b</sup> <i>P</i> <0.0005 compared to CTRL animals				

## References

- Alon, U. (2003). Biological networks: the tinkerer as an engineer. *Science* *301*, 1866–1867.
- Ashburner, M., Ball, C.A., Blake, J.A., Botstein, D., Butler, H., Cherry, J.M., Davis, A.P., Dolinski, K., Dwight, S.S., Eppig, J.T., et al. (2000). Gene ontology: tool for the unification of biology. The Gene Ontology Consortium. *Nat. Genet.* *25*, 25–29.
- Baburina, I., and Jackowski, S. (1999). Cellular responses to excess phospholipid. *J. Biol. Chem.* *274*, 9400–9408.
- Bach, J.-F. (2002). The effect of infections on susceptibility to autoimmune and allergic diseases. *N. Engl. J. Med.* *347*, 911–920.
- Baer, A.N., and Wortmann, R.L. (2007). Myotoxicity associated with lipid-lowering drugs. *Curr. Opin. Rheumatol.* *19*, 67–73.
- Barabási, A.-L., and Oltvai, Z.N. (2004). Network biology: understanding the cell's functional organization. *Nat. Rev. Genet.* *5*, 101–113.
- Barbi, J., Pardoll, D., and Pan, F. (2013). Metabolic control of the Treg/Th17 axis. *Immunol. Rev.* *252*, 52–77.
- Battaglia, M., Stabilini, A., and Roncarolo, M.-G. (2005). Rapamycin selectively expands CD4+CD25+FoxP3+ regulatory T cells. *Blood* *105*, 4743–4748.
- Begley, T.P., Kinsland, C., and Strauss, E. (2001). The biosynthesis of coenzyme A in bacteria. *Vitam. Horm.* *61*, 157–171.
- Ben-Nun, A., Wekerle, H., and Cohen, I.R. (1981). The rapid isolation of clonable antigen-specific T lymphocyte lines capable of mediating autoimmune encephalomyelitis. *Eur. J. Immunol.* *11*, 195–199.
- Berge, R.K., Aarsland, A., Bakke, O.M., and Farstad, M. (1983). Hepatic enzymes, CoASH and long-chain acyl-CoA in subcellular fractions as affected by drugs inducing peroxisomes and smooth endoplasmic reticulum. *Int. J. Biochem.* *15*, 191–204.
- Berge, R.K., Hosøy, L.H., and Farstad, M.N. (1984). Influence of dietary status on liver palmitoyl-coa hydrolase, peroxisomal enzymes, coash and long-chain acyl-coa in rats. *Int. J. Biochem.* *16*, 403–410.
- Berod, L., Friedrich, C., Nandan, A., Freitag, J., Hagemann, S., Harmrolfs, K., Sandouk, A., Hesse, C., Castro, C.N., Bähre, H., et al. (2014). De novo fatty acid synthesis controls the fate between regulatory T and T helper 17 cells. *Nat. Med.* *20*, 1327–1333.
- Bian, L., Josefsson, E., Jonsson, I.-M., Verdrengh, M., Ohlsson, C., Bokarewa, M., Tarkowski, A., and Magnusson, M. (2009). Dichloroacetate alleviates development of collagen II-induced arthritis in female DBA/1 mice. *Arthritis Res. Ther.* *11*, R132.
- Bluestone, J.A. (2011). Mechanisms of tolerance. *Immunol. Rev.* *241*, 5–19.

- Bolomini-Vittori, M., Montresor, A., Giagulli, C., Staunton, D., Rossi, B., Martinello, M., Constantin, G., and Laudanna, C. (2009). Regulation of conformer-specific activation of the integrin LFA-1 by a chemokine-triggered Rho signaling module. *Nat. Immunol.* *10*, 185–194.
- Bour-Jordan, H., Esensten, J.H., Martinez-Llordella, M., Penaranda, C., Stumpf, M., and Bluestone, J.A. (2011). Intrinsic and extrinsic control of peripheral T-cell tolerance by costimulatory molecules of the CD28/B7 family. *Immunol. Rev.* *241*, 180–205.
- Branca, D., Scutari, G., and Siliprandi, N. (1984a). Pantethine and pantothenate effect on the CoA content of rat liver. *Int. J. Vitam. Nutr. Res. Int. Z. Vitam.-Ernährungsforschung J. Int. Vitaminol. Nutr.* *54*, 211–216.
- Branca, D., Scutari, G., and Siliprandi, N. (1984b). Pantethine and pantothenate effect on the CoA content of rat liver. *Int. J. Vitam. Nutr. Res. Int. Z. Vitam.-Ernährungsforschung J. Int. Vitaminol. Nutr.* *54*, 211–216.
- Brass, E.P., Tahiliani, A.G., Allen, R.H., and Stabler, S.P. (1990). Coenzyme A metabolism in vitamin B-12-deficient rats. *J. Nutr.* *120*, 290–297.
- Breus, O., Panasyuk, G., Gout, I.T., Filonenko, V., and Nemazanyy, I. (2009). CoA Synthase is in complex with p85 $\alpha$ PI3K and affects PI3K signaling pathway. *Biochem. Biophys. Res. Commun.* *385*, 581–585.
- Breus, O., Panasyuk, G., Gout, I.T., Filonenko, V., and Nemazanyy, I. (2010). CoA Synthase is phosphorylated on tyrosines in mammalian cells, interacts with and is dephosphorylated by Shp2PTP. *Mol. Cell. Biochem.* *335*, 195–202.
- Brunetti, D., Dusi, S., Giordano, C., Lamperti, C., Morbin, M., Fugnanesi, V., Marchet, S., Fagiolari, G., Sibon, O., Moggio, M., et al. (2014). Pantethine treatment is effective in recovering the disease phenotype induced by ketogenic diet in a pantothenate kinase-associated neurodegeneration mouse model. *Brain J. Neurol.* *137*, 57–68.
- Buck, M.D., O’Sullivan, D., and Pearce, E.L. (2015). T cell metabolism drives immunity. *J. Exp. Med.* *212*, 1345–1360.
- Bulek, A.M., Cole, D.K., Skowera, A., Dolton, G., Gras, S., Madura, F., Fuller, A., Miles, J.J., Gostick, E., Price, D.A., et al. (2012). Structural basis for the killing of human beta cells by CD8(+) T cells in type 1 diabetes. *Nat. Immunol.* *13*, 283–289.
- Caenepeel, S., Charyczak, G., Sudarsanam, S., Hunter, T., and Manning, G. (2004). The mouse kinome: discovery and comparative genomics of all mouse protein kinases. *Proc. Natl. Acad. Sci. U. S. A.* *101*, 11707–11712.
- Cai, L., Sutter, B.M., Li, B., and Tu, B.P. (2011). Acetyl-CoA Induces Cell Growth and Proliferation by Promoting the Acetylation of Histones at Growth Genes. *Mol. Cell* *42*, 426–437.
- Chang, C.-H., Curtis, J.D., Maggi, L.B., Faubert, B., Villarino, A.V., O’Sullivan, D., Huang, S.C.-C., van der Windt, G.J.W., Blagih, J., Qiu, J., et al. (2013). Posttranscriptional control of T cell effector function by aerobic glycolysis. *Cell* *153*, 1239–1251.

- Cheadle, C., Vawter, M.P., Freed, W.J., and Becker, K.G. (2003). Analysis of microarray data using Z score transformation. *J. Mol. Diagn. JMD* 5, 73–81.
- Cighetti, G., Del Puppo, M., Paroni, R., Fiorica, E., and Galli Kienle, M. (1987). Pantethine inhibits cholesterol and fatty acid syntheses and stimulates carbon dioxide formation in isolated rat hepatocytes. *J. Lipid Res.* 28, 152–161.
- Compston, A., and Coles, A. (2008). Multiple sclerosis. *Lancet Lond. Engl.* 372, 1502–1517.
- Corkey, B.E., Hale, D.E., Glennon, M.C., Kelley, R.I., Coates, P.M., Kilpatrick, L., and Stanley, C.A. (1988). Relationship between unusual hepatic acyl coenzyme A profiles and the pathogenesis of Reye syndrome. *J. Clin. Invest.* 82, 782–788.
- Cornille, E., Abou-Hamdan, M., Khrestchatisky, M., Nieoullon, A., de Reggi, M., and Gharib, B. (2010). Enhancement of L-3-hydroxybutyryl-CoA dehydrogenase activity and circulating ketone body levels by pantethine. Relevance to dopaminergic injury. *BMC Neurosci.* 11, 51.
- Dendrou, C.A., Fugger, L., and Friese, M.A. (2015). Immunopathology of multiple sclerosis. *Nat. Rev. Immunol.* 15, 545–558.
- Dusi, S., Valletta, L., Haack, T.B., Tsuchiya, Y., Venco, P., Pasqualato, S., Goffrini, P., Tigano, M., Demchenko, N., Wieland, T., et al. (2014). Exome sequence reveals mutations in CoA synthase as a cause of neurodegeneration with brain iron accumulation. *Am. J. Hum. Genet.* 94, 11–22.
- Evans, M., Rumberger, J.A., Azumano, I., Napolitano, J.J., Citrolo, D., and Kamiya, T. (2014). Pantethine, a derivative of vitamin B5, favorably alters total, LDL and non-HDL cholesterol in low to moderate cardiovascular risk subjects eligible for statin therapy: a triple-blinded placebo and diet-controlled investigation. *Vasc. Health Risk Manag.* 10, 89–100.
- Freitag, J., Berod, L., Kamradt, T., and Sparwasser, T. (2016). Immunometabolism and autoimmunity. *Immunol. Cell Biol.* 94, 925–934.
- Gerriets, V.A., and Rathmell, J.C. (2012). Metabolic pathways in T cell fate and function. *Trends Immunol.* 33, 168–173.
- Gerriets, V.A., Kishton, R.J., Nichols, A.G., Macintyre, A.N., Inoue, M., Ilkayeva, O., Winter, P.S., Liu, X., Priyadharshini, B., Slawinska, M.E., et al. (2015). Metabolic programming and PDHK1 control CD4<sup>+</sup> T cell subsets and inflammation. *J. Clin. Invest.* 125, 194–207.
- van Gijssel-Bonnello, M., Acar, N., Molino, Y., Bretillon, L., Khrestchatisky, M., de Reggi, M., and Gharib, B. (2015). Pantethine Alters Lipid Composition and Cholesterol Content of Membrane Rafts, With Down-Regulation of CXCL12-Induced T Cell Migration. *J. Cell. Physiol.* 230, 2415–2425.
- Gold, R., Linington, C., and Lassmann, H. (2006). Understanding pathogenesis and therapy of multiple sclerosis via animal models: 70 years of merits and culprits in experimental autoimmune encephalomyelitis research. *Brain J. Neurol.* 129, 1953–1971.

- Goss, P.J.E., and Peccoud, J. (1998). Quantitative modeling of stochastic systems in molecular biology by using stochastic Petri nets. *Proc. Natl. Acad. Sci.* *95*, 6750–6755.
- Gudkova, D., Panasyuk, G., Nemazanyy, I., Zhyvoloup, A., Monteil, P., Filonenko, V., and Gout, I. (2012). EDC4 interacts with and regulates the dephospho-CoA kinase activity of CoA synthase. *FEBS Lett.* *586*, 3590–3595.
- Hahn, M., Nicholson, M.J., Pyrdol, J., and Wucherpfennig, K.W. (2005). Unconventional topology of self peptide-major histocompatibility complex binding by a human autoimmune T cell receptor. *Nat. Immunol.* *6*, 490–496.
- Hasin, Y., Seldin, M., and Lusic, A. (2017). Multi-omics approaches to disease. *Genome Biol.* *18*, 83.
- Horejsi, V., and Hrdinka, M. (2014). Membrane microdomains in immunoreceptor signaling. *FEBS Lett.* *588*, 2392–2397.
- Horie, S., Isobe, M., and Suga, T. (1986). Changes in CoA pools in hepatic peroxisomes of the rat under various conditions. *J. Biochem. (Tokyo)* *99*, 1345–1352.
- Hörtnagel, K., Prokisch, H., and Meitinger, T. (2003). An isoform of hPANK2, deficient in pantothenate kinase-associated neurodegeneration, localizes to mitochondria. *Hum. Mol. Genet.* *12*, 321–327.
- Horváth, Z., and Vécsei, L. (2009). Current medical aspects of pantethine. *Ideggyogyaszati Szle.* *62*, 220–229.
- Hotamisligil, G.S. (2017). Foundations of Immunometabolism and Implications for Metabolic Health and Disease. *Immunity* *47*, 406–420.
- Huang, D.W., Sherman, B.T., and Lempicki, R.A. (2009a). Bioinformatics enrichment tools: paths toward the comprehensive functional analysis of large gene lists. *Nucleic Acids Res.* *37*, 1–13.
- Huang, D.W., Sherman, B.T., and Lempicki, R.A. (2009b). Systematic and integrative analysis of large gene lists using DAVID bioinformatics resources. *Nat. Protoc.* *4*, 44–57.
- Ideker, T., Galitski, T., and Hood, L. (2001). A new approach to decoding life: systems biology. *Annu. Rev. Genomics Hum. Genet.* *2*, 343–372.
- Kanehisa, M., and Goto, S. (2000). KEGG: kyoto encyclopedia of genes and genomes. *Nucleic Acids Res.* *28*, 27–30.
- Kanehisa, M., Goto, S., Sato, Y., Kawashima, M., Furumichi, M., and Tanabe, M. (2014). Data, information, knowledge and principle: back to metabolism in KEGG. *Nucleic Acids Res.* *42*, D199–205.
- Karnovsky, A., Weymouth, T., Hull, T., Tarcea, V.G., Scardoni, G., Laudanna, C., Sartor, M.A., Stringer, K.A., Jagadish, H.V., Burant, C., et al. (2012). Metscape 2 bioinformatics tool for the analysis and visualization of metabolomics and gene expression data. *Bioinforma. Oxf. Engl.* *28*, 373–380.

- Kerbey, A.L., Radcliffe, P.M., and Randle, P.J. (1977). Diabetes and the control of pyruvate dehydrogenase in rat heart mitochondria by concentration ratios of adenosine triphosphate/adenosine diphosphate, of reduced/oxidized nicotinamide-adenine dinucleotide and of acetyl-coenzyme A/coenzyme A. *Biochem. J.* *164*, 509–519.
- Kim, J.M., Rasmussen, J.P., and Rudensky, A.Y. (2007). Regulatory T cells prevent catastrophic autoimmunity throughout the lifespan of mice. *Nat. Immunol.* *8*, 191–197.
- Kleinkauf, H. (2000). The role of 4'-phosphopantetheine in the biosynthesis of fatty acids, polyketides and peptides. *BioFactors Oxf. Engl.* *11*, 91–92.
- Korade, Z., and Kenworthy, A.K. (2008). Lipid rafts, cholesterol, and the brain. *Neuropharmacology* *55*, 1265–1273.
- Lango Allen, H., Estrada, K., Lettre, G., Berndt, S.I., Weedon, M.N., Rivadeneira, F., Willer, C.J., Jackson, A.U., Vedantam, S., Raychaudhuri, S., et al. (2010). Hundreds of variants clustered in genomic loci and biological pathways affect human height. *Nature* *467*, 832–838.
- Leitinger, B., and Hogg, N. (2002). The involvement of lipid rafts in the regulation of integrin function. *J. Cell Sci.* *115*, 963–972.
- Leonardi, R., and Jackowski, S. (2007). Biosynthesis of Pantothenic Acid and Coenzyme A. *EcoSal Plus* *2*.
- Leonardi, R., Zhang, Y.-M., Rock, C.O., and Jackowski, S. (2005). Coenzyme A: back in action. *Prog. Lipid Res.* *44*, 125–153.
- Li, J., Zhang, Z., Rosenzweig, J., Wang, Y.Y., and Chan, D.W. (2002). Proteomics and bioinformatics approaches for identification of serum biomarkers to detect breast cancer. *Clin. Chem.* *48*, 1296–1304.
- Lochner, M., Berod, L., and Sparwasser, T. (2015). Fatty acid metabolism in the regulation of T cell function. *Trends Immunol.* *36*, 81–91.
- Lundby, A., Lage, K., Weinert, B.T., Bekker-Jensen, D.B., Secher, A., Skovgaard, T., Kelstrup, C.D., Dmytriyev, A., Choudhary, C., Lundby, C., et al. (2012). Proteomic Analysis of Lysine Acetylation Sites in Rat Tissues Reveals Organ Specificity and Subcellular Patterns. *Cell Rep.* *2*, 419–431.
- MacIver, N.J., Michalek, R.D., and Rathmell, J.C. (2013). Metabolic regulation of T lymphocytes. *Annu. Rev. Immunol.* *31*, 259–283.
- Mak, T.W., Grusdat, M., Duncan, G.S., Dostert, C., Nonnenmacher, Y., Cox, M., Binsfeld, C., Hao, Z., Brüstle, A., Itsumi, M., et al. (2017). Glutathione Primes T Cell Metabolism for Inflammation. *Immunity* *46*, 675–689.
- Manning, G., Plowman, G.D., Hunter, T., and Sudarsanam, S. (2002). Evolution of protein kinase signaling from yeast to man. *Trends Biochem. Sci.* *27*, 514–520.
- Martinez, D.L., Tsuchiya, Y., and Gout, I. (2014). Coenzyme A biosynthetic machinery in mammalian cells. *Biochem. Soc. Trans.* *42*, 1112–1117.

- McAllister, R.A., Fixter, L.M., and Campbell, E.H. (1988). The effect of tumour growth on liver pantothenate, CoA, and fatty acid synthetase activity in the mouse. *Br. J. Cancer* *57*, 83–86.
- McRae, M.P. (2005). Treatment of hyperlipoproteinemia with pantethine: a review and analysis of efficacy and tolerability. *PubMed Health*.
- Merico, D., Isserlin, R., Stueker, O., Emili, A., and Bader, G.D. (2010). Enrichment Map: A Network-Based Method for Gene-Set Enrichment Visualization and Interpretation. *PLoS ONE* *5*.
- Michalek, R.D., Gerriets, V.A., Jacobs, S.R., Macintyre, A.N., MacIver, N.J., Mason, E.F., Sullivan, S.A., Nichols, A.G., and Rathmell, J.C. (2011). Cutting edge: distinct glycolytic and lipid oxidative metabolic programs are essential for effector and regulatory CD4<sup>+</sup> T cell subsets. *J. Immunol. Baltim. Md 1950* *186*, 3299–3303.
- Miller, S.D., Turley, D.M., and Podojil, J.R. (2007). Antigen-specific tolerance strategies for the prevention and treatment of autoimmune disease. *Nat. Rev. Immunol.* *7*, 665.
- Nathan, C., and Cunningham-Bussell, A. (2013). Beyond oxidative stress: an immunologist's guide to reactive oxygen species. *Nat. Rev. Immunol.* *13*, 349–361.
- Nemazanyy, I., Panasyuk, G., Zhyvoloup, A., Panayotou, G., Gout, I.T., and Filonenko, V. (2004). Specific interaction between S6K1 and CoA synthase: a potential link between the mTOR/S6K pathway, CoA biosynthesis and energy metabolism. *FEBS Lett.* *578*, 357–362.
- O'Neill, L.A.J., Kishton, R.J., and Rathmell, J. (2016). A guide to immunometabolism for immunologists. *Nat. Rev. Immunol.* *16*, 553–565.
- Ortiz, G.G., Pacheco-Moisés, F.P., Macías-Islas, M.Á., Flores-Alvarado, L.J., Mireles-Ramírez, M.A., González-Renovato, E.D., Hernández-Navarro, V.E., Sánchez-López, A.L., and Alatorre-Jiménez, M.A. (2014). Role of the blood-brain barrier in multiple sclerosis. *Arch. Med. Res.* *45*, 687–697.
- O'Sullivan, D., and Pearce, E.L. (2015). Targeting T cell metabolism for therapy. *Trends Immunol.* *36*, 71–80.
- Palsson-McDermott, E.M., Curtis, A.M., Goel, G., Lauterbach, M.A., Sheedy, F.J., Gleeson, L.E., van den Bosch, M.W., Quinn, S.R., Domingo-Fernandez, R., Johnson, D.G., et al. (2015). Pyruvate Kinase M2 regulates Hif-1 $\alpha$  activity and IL-1 $\beta$  induction, and is a critical determinant of the Warburg Effect in LPS-activated macrophages. *Cell Metab.* *21*, 65–80.
- Pastrello, C., Pasini, E., Kotlyar, M., Otasek, D., Wong, S., Sangrar, W., Rahmati, S., and Jurisica, I. (2014). Integration, visualization and analysis of human interactome. *Biochem. Biophys. Res. Commun.* *445*, 757–773.
- Patel, C.H., and Powell, J.D. (2017). Targeting T cell metabolism to regulate T cell activation, differentiation and function in disease. *Curr. Opin. Immunol.* *46*, 82–88.
- Păun, G. (2000). Computing with Membranes. *J. Comput. Syst. Sci.* *61*, 108–143.



- Pearce, E.L., and Pearce, E.J. (2013). Metabolic pathways in immune cell activation and quiescence. *Immunity* 38, 633–643.
- Pearce, E.L., Poffenberger, M.C., Chang, C.-H., and Jones, R.G. (2013). Fueling immunity: insights into metabolism and lymphocyte function. *Science* 342, 1242454.
- Penet, M.-F., Abou-Hamdan, M., Coltel, N., Cornille, E., Grau, G.E., de Reggi, M., and Gharib, B. (2008). Protection against cerebral malaria by the low-molecular-weight thiol pantethine. *Proc. Natl. Acad. Sci. U. S. A.* 105, 1321–1326.
- Petermann, F., and Korn, T. (2011). Cytokines and effector T cell subsets causing autoimmune CNS disease. *FEBS Lett.* 585, 3747–3757.
- Piccio, L., Rossi, B., Scarpini, E., Laudanna, C., Giagulli, C., Issekutz, A.C., Vestweber, D., Butcher, E.C., and Constantin, G. (2002). Molecular mechanisms involved in lymphocyte recruitment in inflamed brain microvessels: critical roles for P-selectin glycoprotein ligand-1 and heterotrimeric G(i)-linked receptors. *J. Immunol. Baltim. Md 1950* 168, 1940–1949.
- Pihl-Jensen, G., Tsakiri, A., and Frederiksen, J.L. (2015). Statin treatment in multiple sclerosis: a systematic review and meta-analysis. *CNS Drugs* 29, 277–291.
- Powell, J.D., Lerner, C.G., and Schwartz, R.H. (1999). Inhibition of cell cycle progression by rapamycin induces T cell clonal anergy even in the presence of costimulation. *J. Immunol. Baltim. Md 1950* 162, 2775–2784.
- Rana, A., Seinen, E., Siudeja, K., Muntendam, R., Srinivasan, B., van der Want, J.J., Hayflick, S., Reijngoud, D.-J., Kayser, O., and Sibon, O.C.M. (2010). Pantethine rescues a *Drosophila* model for pantothenate kinase-associated neurodegeneration. *Proc. Natl. Acad. Sci. U. S. A.* 107, 6988–6993.
- Rangachari, M., and Kuchroo, V.K. (2013). Using EAE to better understand principles of immune function and autoimmune pathology. *J. Autoimmun.* 45, 31–39.
- Rathmell, J.C., Vander Heiden, M.G., Harris, M.H., Frauwirth, K.A., and Thompson, C.B. (2000). In the absence of extrinsic signals, nutrient utilization by lymphocytes is insufficient to maintain either cell size or viability. *Mol. Cell* 6, 683–692.
- Regev, A., Silverman, W., and Shapiro, E. (2001). Representation and simulation of biochemical processes using the pi-calculus process algebra. *Pac. Symp. Biocomput. Pac. Symp. Biocomput.* 459–470.
- Reibel, D.K., Wyse, B.W., Berkich, D.A., Palko, W.M., and Neely, J.R. (1981). Effects of diabetes and fasting on pantothenic acid metabolism in rats. *Am. J. Physiol.* 240, E597-601.
- Reibel, D.K., Uboh, C.E., and Kent, R.L. (1983). Altered coenzyme A and carnitine metabolism in pressure-overload hypertrophied hearts. *Am. J. Physiol.* 244, H839-843.
- Reijonen, H., Novak, E.J., Kochik, S., Heninger, A., Liu, A.W., Kwok, W.W., and Nepom, G.T. (2002). Detection of GAD65-specific T-cells by major histocompatibility complex class II tetramers in type 1 diabetic patients and at-risk subjects. *Diabetes* 51, 1375–1382.

- Robishaw, J.D., Berkich, D., and Neely, J.R. (1982). Rate-limiting step and control of coenzyme A synthesis in cardiac muscle. *J. Biol. Chem.* *257*, 10967–10972.
- Rock, C.O., Calder, R.B., Karim, M.A., and Jackowski, S. (2000). Pantothenate kinase regulation of the intracellular concentration of coenzyme A. *J. Biol. Chem.* *275*, 1377–1383.
- Roos, D., and Loos, J.A. (1973). Changes in the carbohydrate metabolism of mitogenically stimulated human peripheral lymphocytes: II. Relative importance of glycolysis and oxidative phosphorylation on phytohaemagglutinin stimulation. *Exp. Cell Res.* *77*, 127–135.
- Rossi, B., Angiari, S., Zenaro, E., Budui, S.L., and Constantin, G. (2011). Vascular inflammation in central nervous system diseases: adhesion receptors controlling leukocyte-endothelial interactions. *J. Leukoc. Biol.* *89*, 539–556.
- Rumberger, J.A., Napolitano, J., Azumano, I., Kamiya, T., and Evans, M. (2011). Pantethine, a derivative of vitamin B(5) used as a nutritional supplement, favorably alters low-density lipoprotein cholesterol metabolism in low- to moderate-cardiovascular risk North American subjects: a triple-blinded placebo and diet-controlled investigation. *Nutr. Res. N. Y. N* *31*, 608–615.
- Shannon, P., Markiel, A., Ozier, O., Baliga, N.S., Wang, J.T., Ramage, D., Amin, N., Schwikowski, B., and Ideker, T. (2003). Cytoscape: a software environment for integrated models of biomolecular interaction networks. *Genome Res.* *13*, 2498–2504.
- Shi, L.Z., Wang, R., Huang, G., Vogel, P., Neale, G., Green, D.R., and Chi, H. (2011). HIF1 $\alpha$ -dependent glycolytic pathway orchestrates a metabolic checkpoint for the differentiation of Th17 and Treg cells. *J. Exp. Med.* *208*, 1367–1376.
- Sibon, O.C.M., and Strauss, E. (2016). Coenzyme A: to make it or uptake it?
- Sigal, N.H., and Dumont, F.J. (1992). Cyclosporin A, FK-506, and Rapamycin: Pharmacologic Probes of Lymphocyte Signal Transduction. *Annu. Rev. Immunol.* *10*, 519–560.
- Siudeja, K., Srinivasan, B., Xu, L., Rana, A., de Jong, J., Nollen, E.A.A., Jackowski, S., Sanford, L., Hayflick, S., and Sibon, O.C.M. (2011). Impaired Coenzyme A metabolism affects histone and tubulin acetylation in *Drosophila* and human cell models of pantothenate kinase associated neurodegeneration. *EMBO Mol. Med.* *3*, 755–766.
- Smith, C.M., and Savage, C.R. (1980). Regulation of coenzyme A biosynthesis by glucagon and glucocorticoid in adult rat liver parenchymal cells. *Biochem. J.* *188*, 175–184.
- Steinman, L. (1999). Assessment of animal models for MS and demyelinating disease in the design of rational therapy. *Neuron* *24*, 511–514.
- Su, L.F., Kidd, B.A., Han, A., Kotzin, J.J., and Davis, M.M. (2013). Virus-specific CD4(+) memory-phenotype T cells are abundant in unexposed adults. *Immunity* *38*, 373–383.

- Sukhatme, V.P., and Chan, B. (2012). Glycolytic cancer cells lacking 6-phosphogluconate dehydrogenase metabolize glucose to induce senescence. *FEBS Lett.* *586*, 2389–2395.
- Szklarczyk, D., Morris, J.H., Cook, H., Kuhn, M., Wyder, S., Simonovic, M., Santos, A., Doncheva, N.T., Roth, A., Bork, P., et al. (2017). The STRING database in 2017: quality-controlled protein-protein association networks, made broadly accessible. *Nucleic Acids Res.* *45*, D362–D368.
- Thomas, A.G., O’Driscoll, C.M., Bressler, J., Kaufmann, W., Rojas, C.J., and Slusher, B.S. (2014). Small molecule glutaminase inhibitors block glutamate release from stimulated microglia. *Biochem. Biophys. Res. Commun.* *443*, 32–36.
- Vander Heiden, M.G., Cantley, L.C., and Thompson, C.B. (2009). Understanding the Warburg effect: the metabolic requirements of cell proliferation. *Science* *324*, 1029–1033.
- Vidal, M., Cusick, M.E., and Barabási, A.-L. (2011). Interactome Networks and Human Disease. *Cell* *144*, 986–998.
- Waickman, A.T., and Powell, J.D. (2012). mTOR integrates diverse inputs to guide the outcome of antigen recognition in T cells. *J. Immunol. Baltim. Md 1950* *188*, 4721–4729.
- Wingerchuk, D.M., and Carter, J.L. (2014). Multiple sclerosis: current and emerging disease-modifying therapies and treatment strategies. *Mayo Clin. Proc.* *89*, 225–240.
- Winterhalter, C., Widera, P., and Krasnogor, N. (2014). JEPETTO: a Cytoscape plugin for gene set enrichment and topological analysis based on interaction networks. *Bioinformatics* *30*, 1029–1030.
- Wittwer, C.T., Gahl, W.A., Butler, J.D., Zatz, M., and Thoene, J.G. (1985). Metabolism of pantethine in cystinosis. *J. Clin. Invest.* *76*, 1665–1672.
- Wolf, A.J., Reyes, C.N., Liang, W., Becker, C., Shimada, K., Wheeler, M.L., Cho, H.C., Popescu, N.I., Coggeshall, K.M., Arditi, M., et al. (2016). Hexokinase Is an Innate Immune Receptor for the Detection of Bacterial Peptidoglycan. *Cell* *166*, 624–636.
- Wucherpfennig, K.W., Zhang, J., Witek, C., Matsui, M., Modabber, Y., Ota, K., and Hafler, D.A. (1994). Clonal expansion and persistence of human T cells specific for an immunodominant myelin basic protein peptide. *J. Immunol.* *152*, 5581–5592.
- Wucherpfennig, K.W., Call, M.J., Deng, L., and Mariuzza, R. (2009). Structural Alterations in peptide–MHC Recognition by Self-reactive T cell Receptors. *Curr. Opin. Immunol.* *21*, 590–595.
- Yang, Z., Matteson, E.L., Goronzy, J.J., and Weyand, C.M. (2015). T-cell metabolism in autoimmune disease. *Arthritis Res. Ther.* *17*, 29.
- Zamvil, S.S., and Steinman, L. (1990). The T lymphocyte in experimental allergic encephalomyelitis. *Annu. Rev. Immunol.* *8*, 579–621.
- Zhang, L., Nakayama, M., and Eisenbarth, G.S. (2008). Insulin as an autoantigen in NOD/human diabetes. *Curr. Opin. Immunol.* *20*, 111–118.

Zhou, B., Westaway, S.K., Levinson, B., Johnson, M.A., Gitschier, J., and Hayflick, S.J. (2001). A novel pantothenate kinase gene (PANK2) is defective in Hallervorden-Spatz syndrome. *Nat. Genet.* 28, 345–349.

Zhyvoloup, A., Nemazanyy, I., Panasyuk, G., Valovka, T., Fenton, T., Rebholz, H., Wang, M.-L., Foxon, R., Lyzogubov, V., Usenko, V., et al. (2003). Subcellular localization and regulation of coenzyme A synthase. *J. Biol. Chem.* 278, 50316–50321.